

Selection of functional predictors and smooth coefficient estimation for scalar-on-function regression models

Hedayat Fathi

Department of Operations and Decision Systems, Université Laval, Québec, Canada

hedayat.fathi.1@ulaval.ca

Marzia A. Cremona

Department of Operations and Decision Systems, Université Laval, Québec, Canada

marzia.cremona@fsa.ulaval.ca

Federico Severino

Department of Finance, Insurance and Real Estate, Université Laval, Québec, Canada

federico.severino@fsa.ulaval.ca

Abstract

In the framework of scalar-on-function regression models, in which several functional variables are employed to predict a scalar response, we propose a methodology for selecting relevant functional predictors while simultaneously providing accurate smooth (or, more generally, regular) estimates of the functional coefficients. We suppose that the functional predictors belong to a real separable Hilbert space, while the functional coefficients belong to a specific subspace of this Hilbert space. Such a subspace can be a Reproducing Kernel Hilbert Space (RKHS) to ensure the desired regularity characteristics, such as smoothness or periodicity, for the coefficient estimates. Our procedure, called SOFIA (Scalar-On-Function Integrated Adaptive Lasso), is based on an adaptive penalized least squares algorithm that leverages functional subgradients to efficiently solve the minimization problem. We demonstrate that the proposed method satisfies the functional oracle property, even when the number of predictors exceeds the sample size. SOFIA's effectiveness in variable selection and coefficient estimation is evaluated through extensive simulation studies and a real-data application to GDP growth prediction.

Keywords: Variable Selection, Scalar-on-Function Regression, Functional Data Analysis, Reproducing Kernel Hilbert Spaces, Regularization, Oracle Property

1 Introduction

High-dimensional regression models are at the core of contemporary data analysis, with many applications in various fields, including genetics, finance, and social sciences. A key development in this context is the use of functional data, where some or all variables are not scalar variables but functions that vary over a continuum, such as time or space. Functional data offer advantages, particularly by enabling the application of functional analysis techniques, which can result in more accurate data analyses, improved pattern extraction, and enhanced visualization. However, they also introduce new challenges in statistical modeling, especially when dealing with a large set of functional predictors. Selecting the most relevant ones is crucial to reduce computational complexity, improve model interpretability, and improve predictive accuracy. As standard references for functional data analysis (FDA) we refer to Ramsay and Silverman (2005) and Kokoszka and Reimherr (2017).

Functional linear regression models can be classified into three categories: scalar response with functional predictors, functional response with scalar predictors, and functional response with functional predictors. In our study, we focus on the first category, known as scalar-on-function regressions, and introduce a new approach that simultaneously performs variable selection and yields smooth estimations of coefficients. We consider the standardized regression model

$$Y_n = \sum_{i=1}^I \langle \beta_i^*, X_{ni} \rangle_{\mathbb{H}} + \epsilon_n, \quad n = 1, \dots, N, \quad (1)$$

where Y_n is the scalar response for the subject n , the functional predictors X_{ni} are in a real separable Hilbert space $(\mathbb{H}, \langle \cdot, \cdot \rangle_{\mathbb{H}})$ (in many cases $L^2[0, 1]$), and the scalars ϵ_n are independent random errors with mean 0 and variance σ^2 . For each i , the function β_i^* quantifies the effect of the i^{th} functional predictor on the scalar response. Applications of scalar-on-function regression are widespread, including finance (where curves represent time series), medicine, and the natural sciences. See Ullah and Finch (2013) for a systematic review of applications of functional linear regression and, more broadly, FDA.

Although variable selection methods for classic linear regression models are ubiquitous in the statistical literature, these methods have been considered only recently in the functional setting. For a review of recent studies in the functional setting, we refer to Aneiros et al. (2022), and for classic regression models, we refer to Insolia et al. (2022) and Hanke et al. (2024).

In this paper, we focus on situations where there are multiple functional predictors but only some are significant. The number of variables and the number of active ones may increase with the sample size. Specifically, we allow the number of predictors to grow faster than the sample size (even at an exponential rate). The challenges of such situations in multiple regression models are illustrated in Huang et al. (2008). “Best subset selection” may be computationally infeasible, “stepwise selection” often provides only locally optimal solutions, and Lasso does not satisfy the oracle property (Fan and Li, 2001).

Here, we propose an adaptive Lasso method that simultaneously performs variable selection and ensures a specified level of smoothness for the coefficient functions. To avoid redundancy in terminology, we refer to our approach as SOFIA-Lasso (Scalar-On-Function Integrated Adaptive Lasso) or, for short, SOFIA. The term “integrated” reflects the integration of two norms, enabling the simultaneous selection of variables and regularization of functional coefficients.

The adaptive Lasso method is introduced in the classic multivariate regression by Zou (2006). It adds a data-driven weighting scheme to the penalty term to improve the accuracy of the estimates.

For the first step, (non-adaptive) Lasso can be used to obtain the initial estimates of the coefficients. Then, in the second step, the weights are set as reciprocals of the absolute values of these estimates. The primary challenge in the scalar-on-function setting is that the design matrix does not consist of scalar entries but contains elements from a Hilbert space. This difference introduces several computational and theoretical challenges that need to be addressed.

In our approach, while predictors belong to a general Hilbert space \mathbb{H} , we assume that coefficient functions β_i^* belong to a specific dense Hilbert subspace \mathbb{K} that incorporates desirable properties such as smoothness or periodicity. This subspace is defined by the eigenfunctions of a positive self-adjoint operator K on \mathbb{H} . When a positive-definite kernel induces the operator K , the resulting space forms a reproducing kernel Hilbert space (RKHS): see Hsing and Eubank (2015) for definitions. So, our framework generalizes RKHS settings, offering greater flexibility in selecting the underlying function space. This assumption achieves two primary objectives. First, it ensures a desired level of regularity for the coefficient functions β_i^* . Choosing the operator K appropriately, we can control the smoothness level of the coefficients. This provides tailored regularization strategies to address the specific needs of various applications. Second, this assumption, together with the decay properties of the eigenvalues of the operator K , facilitates the approximation of the objective function within finite-dimensional subspaces while ensuring that the approximation error remains uniformly bounded.

The Hilbert spaces \mathbb{H} and \mathbb{K} share the same orthonormal basis, consisting of the eigenfunctions of K . In other words, \mathbb{H} and \mathbb{K} are defined on the same algebraic structure, but the topology of \mathbb{K} is finer and induces a stronger norm than that of \mathbb{H} . This distinction allows us to define the objective function of SOFIA as the following penalized least squares estimator of the coefficients in eq. (1).

$$\hat{\beta} = \operatorname{argmin}_{\beta \in \mathbb{K}^I} \frac{1}{2N} \sum_{n=1}^N \left(Y_n - \sum_{i=1}^I \langle \beta_i, X_{ni} \rangle_{\mathbb{H}} \right)^2 + \lambda \sum_{i=1}^I \tilde{w}_i \|\beta_i\|_{\mathbb{K}}, \quad (2)$$

where λ is a tuning parameter and \tilde{w}_i are adaptive weights designed to penalize smaller coefficient norms more heavily.

A crucial challenge in the study of functional regression models is the infinite-dimensional nature of the problem. This issue is particularly pronounced in scalar-on-function regressions because the covariance matrix contains finite-rank operators on \mathbb{H} . Consequently, the dimension of the underlying space always exceeds the rank of the covariance matrix, so this matrix (and its restrictions to the space of true predictors) can never be injective as an operator. To address this issue, a common approach in the literature is to project the predictors onto a finite-dimensional subspace of \mathbb{H} , denoted by $\mathbb{H}^{(m)}$. This subspace is defined by an orthonormal basis, which may be predefined (e.g., splines), data driven (e.g., functional principal components), or derived from a general basis (Roche, 2023). In this paper, the basis is derived from the eigenfunctions of the operator K , allowing us to project both functional predictors and coefficient functions onto the subspaces $\mathbb{H}^{(m)}$ and $\mathbb{K}^{(m)}$, respectively. This leads to the following finite-dimensional approximation of (2) on the space $\mathbb{K}^{(m)}$:

$$\hat{\beta}^{(m)} = \operatorname{argmin}_{\beta \in \mathbb{K}^{(m)I}} \frac{1}{2N} \sum_{n=1}^N \left(Y_n - \sum_{i=1}^I \langle \beta_i, X_{ni}^{(m)} \rangle_{\mathbb{H}} \right)^2 + \lambda \sum_{i=1}^I \tilde{w}_i \|\beta_i\|_{\mathbb{K}}. \quad (3)$$

We prove that the approximation error uniformly converges to zero under some mild conditions, like having a bounded design. This result enables us to analyze the asymptotic properties of the estimators.

1.1 Our contributions

The objective of this paper is to introduce a method for variable selection in scalar-on-function regression models that ensures the regularity of the estimated coefficients while satisfying the functional oracle property. We start with the estimator (3) where the weights \tilde{w}_j are set to 1 and prove that under an appropriate version of the restricted eigenvalue (RE) condition, the estimation error admits a sharp bound. This bound provides a rigorous starting point for the adaptive step. A similar result has previously been established for the scalar design in Barber et al. (2017), but our proof is novel when the predictors are finite-dimensional truncations of functional data, i.e., vectors.

The main theorem (i.e. Theorem 2) proves the functional oracle property of SOFIA in the sense of Fan and Reimherr (2017). We prove that SOFIA correctly identifies the true predictors with probability tending to one under some appropriate assumptions on the finite-dimensional projections. Moreover, if the projections of the true coefficients on $\mathbb{H}^{(m)}$ converge to the original coefficients at a sufficiently fast rate, then the estimation error satisfies $o_P(n^{-1/2})$ in the \mathbb{K} -norm. We derive all asymptotic results in the topology of \mathbb{K} . Since this topology is stronger than that of \mathbb{H} , the results also hold in the topology of \mathbb{H} . This responds to an open question posed by Parodi and Reimherr (2018).

Another major contribution of ours is the comparative analysis of variable selection and estimation performance across several recent methods using multiple simulation scenarios. We compare the performance of SOFIA with the standard group Lasso (Fan et al., 2015), the semi-adaptive and adaptive group Lasso (Gertheiss et al., 2013), as well as the approaches proposed in Roche (2023) and Boschi et al. (2024).

Finally, we analyze a real-world dataset that is novel in its own right. We consider a financial dataset that contains several variables relevant to forecasting Canadian GDP growth. This application presents several challenges, such as handling unbalanced data and high-frequency variables. We address them by representing the predictors as FDA objects. Then, we identify the key predictors to forecast the scalar response of GDP growth.

1.2 Related works

The literature on variable selection for scalar-on-function regression models remains relatively limited, with few studies addressing this problem. This issue was first examined in Cardot et al. (2007) in the context of ozone prediction, where the authors proposed an approach similar to the best subset selection. Since then, most of the existing methods for variable selection in these models have relied on a group modeling strategy (Aneiros et al., 2022), which reformulates the problem as a grouped linear regression model.

In the framework of scalar-on-function regression models, functional predictors are selected or discarded by replacing each of them with a finite set of scalar coefficients. The functional predictors and coefficients belong to a Hilbert space, which allows them to be expanded using a suitable basis system. The expansion is then truncated to obtain a finite-dimensional representation of the problem. The distinctions between existing methods lie in the choice of the basis and of the variable selection technique. For example, Matsui and Konishi (2011) use Gaussian basis functions combined with a penalized least squares approach, while Gertheiss et al. (2013) employ B-spline basis functions with a group Lasso penalty for variable selection. Finally, Lian (2013) and Huang et al. (2016) adopt functional principal components as the basis expansion, using penalized least squares and penalized least absolute deviation, respectively.

Fan et al. (2015) propose an additive regression model that encompasses a broad class of regression frameworks, including linear regression. Their approach allows the number of predictors to exceed the sample size. The study provides a rigorous asymptotic analysis, assuming that all predictors and regression coefficients belong to a Sobolev ellipsoid of order two. However, the assumption that predictors are known a priori to belong to a Sobolev ellipsoid may be considered overly restrictive. Later, Huang et al. (2016) considered a similar setting but employed a data-driven basis derived from functional principal component analysis (FPCA). They also modified the penalty term by using the ℓ_1/ℓ_∞ norm instead of ℓ_1/ℓ_2 . While their approach yields similar analytical results, a key limitation is its computational complexity when the number of predictors is large, as it requires estimating a set of basis functions for each predictor.

To our knowledge, the only reference in the scalar-on-function regression context that considers predictors in a general Hilbert space and examines the asymptotic properties is Roche (2023). The latter demonstrates that the standard RE condition is never satisfied when the predictors belong to an infinite-dimensional space. Roche (2023) introduces a modified RE condition that is compatible with the infinite-dimensional nature of the problem. It is defined as a sequence of scalars, each corresponding to a finite-dimensional approximation of the model. This sequence converges to zero as the truncation dimension increases. We will explore this sequence in greater depth in Section 2. The paper investigates the sharp oracle properties of the proposed method. However, since the prediction and estimation bounds depend on the sample size and the truncation dimension, the bounds diverge to infinity if the dimensionality increases too rapidly. This poses a significant challenge, and the optimal selection of the truncation dimension remains an open problem.

The recent study by Boschi et al. (2024) introduces an adaptive elastic net method for variable selection in function-on-function regression named FASStEN. The authors employ FPCA and a dual augmented Lagrangian approach to establish the oracle property. Although FASStEN is not explicitly designed for scalar-on-function regression, it provides an implementation comparable to SOFIA.

Gertheiss et al. (2013) is the most notable work among those without analytical results. The authors propose two adaptive group Lasso methods incorporating a sparsity-smoothness penalty for variable selection. The penalty term consists of two components controlled by separate parameters: one regulates the overall magnitude of the penalty, while the other enforces smoothness. Although this dual-parameter structure improves the performance of variable selection, it also increases computational complexity. Moreover, similar to other grouping methods, it tends to yield many false positives, particularly when the number of predictors is large.

As mentioned, RKHS play an essential role in our study. RKHS have received considerable attention over the past two decades in linear functional regression models. A seminal contribution in this area was made by Yuan and Cai (2010), who introduced a smoothness regularization method based on RKHS. Since then, RKHS-based approaches have been employed in various FDA studies for different purposes. For the foundational aspects of RKHS in functional regression models, see Kadri et al. (2010), while recent advancements can be found in Wang et al. (2022). In the context of linear regression models based on RKHS, two approaches can be used for parameter estimation: the “representer theorem” and “functional subgradients”. The approach based on the representer theorem is the dominant method in the use of RKHS in linear regression due to its theoretical convenience; see, for example, Yuan and Cai (2010), Shin and Lee (2016), and Berrendero et al. (2019). However, the methods based on the representer theorem tend to be slow (Parodi and Reimherr, 2018). For this reason, in our paper, we will use functional subgradients to find the minimum of the SOFIA objective function.

Finally, it is worth mentioning a series of follow-up papers by Reimherr and coauthors on

variable selection in function-on-scalar linear regressions using Lasso-type regularization. While the context is in the opposite direction of ours, the definition of the oracle property and some ideas on the underlying spaces are borrowed from such studies. Barber et al. (2017) propose a method based on the (unweighted) group Lasso, named FS-Lasso. While the oracle property is not satisfied, they give some reasonable bounds for estimation and prediction errors. Fan and Reimherr (2017) use the reciprocal of the norms of the coefficients obtained in Barber et al. (2017) as weights for the penalty term and prove the (functional) oracle property of the method. Then, Parodi and Reimherr (2018) allows the coefficients to belong to an RKHS. The oracle property is satisfied, and the main advantage is its ability to select relevant variables while ensuring that the coefficients exhibit desired properties such as smoothness or periodicity.

1.3 Organization

Section 2 introduces the framework of our study and outlines the assumptions about the data and the coefficients. Furthermore, it provides the essential mathematical notation and technical assumptions needed for the theoretical analysis. Section 3 presents the main theoretical results. We demonstrate that, given an appropriate starting point, the proposed adaptive Lasso satisfies the functional oracle property. Section 4 details the implementation procedure using the functional subgradient method. Section 5 presents an extensive simulation study that compares the performance of SOFIA with existing approaches. Section 6 provides a real-world case study on identifying significant variables for the prediction of GDP growth.

2 Mathematical framework

This section introduces the mathematical and functional framework that underlies our method. We begin by describing the general structure of the Hilbert space in which the functional predictors are defined and present the assumptions required for the model. These include regularity conditions on the coefficient functions and the structure of the trace-class operator that defines the Hilbert subspace where the coefficients reside. We then provide a structured set of assumptions that ensure the uniform convergence of the estimation procedure.

Consider a general real separable Hilbert space $(\mathbb{H}, \|\cdot\|_{\mathbb{H}})$, where the norm is derived from the inner product $\langle \cdot, \cdot \rangle_{\mathbb{H}}$. We assume that the predictors are elements of \mathbb{H} . Thus, our approach encompasses a wide range of spaces, including the function space $L^2[0, 1]$, Euclidean spaces \mathbb{R}^N , and more specialized function spaces commonly used in statistical learning, such as product spaces, Sobolev spaces, Wiener spaces, and RKHS.

To ensure the selection of important variables and the regularization of the coefficients, we follow the definitions given in Parodi and Reimherr (2018). We consider a (compact) trace-class operator, $K : \mathbb{H} \rightarrow \mathbb{H}$, which is positive definite and self-adjoint. By the spectral theorem for compact self-adjoint operators, K can be decomposed into the form

$$K = \sum_{l=1}^{+\infty} \theta_l v_l \otimes v_l, \quad (4)$$

where $\theta_1 \geq \theta_2 \geq \dots > 0$ are the ordered eigenvalues and $v_i \in \mathbb{H}$ are the corresponding eigenfunctions, which constitute an orthonormal basis for \mathbb{H} (Murphy, 1990, Theorem 2.4.4). The notation $x \otimes y$ denotes the rank-one operator defined by $(x \otimes y)(h) := \langle y, h \rangle_{\mathbb{H}} x$ for any $x, y, h \in \mathbb{H}$. Now,

we define the subspace of \mathbb{H}

$$\mathbb{K} := \left\{ h \in \mathbb{H} : \sum_{l=1}^{+\infty} \frac{|\langle h, v_l \rangle_{\mathbb{H}}|^2}{\theta_l} =: \|h\|_{\mathbb{K}}^2 < +\infty \right\}.$$

Equipped with the norm $\|\cdot\|_{\mathbb{K}}$, \mathbb{K} is itself a Hilbert space. When $\mathbb{H} = L^2[0, 1]$, many examples of the operator K have been introduced in the literature. In particular, if K is defined as an integral operator associated with a kernel function $k(t, s)$, then K is a trace-class, positive, and self-adjoint operator. As a result, any RKHS can be viewed as a special case of a Hilbert space \mathbb{K} . In Section 5, we will introduce a family of operators to implement our method. For a detailed discussion on compact and trace-class operators in Hilbert spaces, we refer to Murphy (1990), Section 2.4. For an overview of various types of kernels, see Berlinet and Thomas-Agnan (2011), Chapter 7.

In our method, the coefficient functions β_j are assumed to belong to the Hilbert space \mathbb{K} . This assumption ensures the desired level of regularity for the coefficients through the choice of an appropriate operator K , and it is essential to establish the oracle property. Here, we study the relation between the spaces \mathbb{K} and \mathbb{H} . This analysis is particularly important, as the penalty term in our model is defined via the \mathbb{K} -norm, whereas the least squares term involves the inner product in \mathbb{H} . As a result, it is necessary to explicitly characterize the relationship between these two norms.

Let $R(K)$ denote the range of the operator K . For any $h \in R(K)$, the range norm of h is defined as

$$\|h\|_{R(K)} = \inf \{ \|g\|_{\mathbb{H}} : K(g) = h \}.$$

It is straightforward to verify that, with this norm, the vector space $R(K)$ becomes a Hilbert space, even though $R(K)$ is never a closed subspace of \mathbb{H} . Since 0 is assumed to not be an eigenvalue of K , the operator K is injective, allowing us to define $\|h\|_{R(K)}$ in terms of the preimage of h . With this formulation, the pair $(R(K), \|\cdot\|_{R(K)})$ ensures that the operator $K : (\mathbb{H}, \|\cdot\|_{\mathbb{H}}) \rightarrow (R(K), \|\cdot\|_{R(K)})$ is a surjective isometry. For further details on the range norm and its connection to RKHS, see Sarason (2007) and Paulsen and Raghupathi (2016). The proof of the proposition is given in Appendix A.1.

The following proposition elucidates the structure of the coefficient space \mathbb{K} by showing that it coincides with the range of $K^{1/2}$. This characterization allows the computation of \mathbb{K} -norms based on \mathbb{H} -norms.

Proposition 1. *If K has the spectral decomposition (4), then the Hilbert space \mathbb{K} coincides with $(R(K^{1/2}), \|\cdot\|_{R(K^{1/2})})$ as a Hilbert space.*

This proposition also demonstrates that the assumption that the coefficients reside in the subspace \mathbb{K} is not overly restrictive. In fact, since all the eigenvalues of K are assumed to be nonzero, the spectral mapping theorem implies that $K^{1/2}$ also has nonzero eigenvalues. Consequently, its null space is zero and its range is dense in \mathbb{H} with respect to the topology induced by the norm of \mathbb{H} .

2.1 Model

The following assumption establishes the foundational framework for our functional linear model by specifying the structure of the response, the predictors, and the coefficient functions.

Assumption 1. Let Y_n denote the scalar response for subject n , and $X_n = (X_{n1}, \dots, X_{nI})$ represent the functional predictors in the Hilbert space \mathbb{H}^I . The coefficient functions $\beta^* = (\beta_1^*, \dots, \beta_I^*)$ belong to the Hilbert subspace $\mathbb{K}^I \subset \mathbb{H}^I$ and satisfy the following functional linear model

$$Y_n = \sum_{i=1}^I \langle \beta_i^*, X_{ni} \rangle_{\mathbb{H}} + \epsilon_n. \quad (5)$$

Moreover, given $I_0 < I$, only the first I_0 predictors are active, which means that the remaining $I - I_0$ predictors do not contribute to Y_n . Consequently, their corresponding coefficients are assumed to be zero. We center the response variable and standardize the predictors so that

$$\sum_{n=1}^N Y_n = 0, \quad \sum_{n=1}^N X_{ni} = 0, \quad \text{and} \quad \frac{1}{N} \sum_{n=1}^N \|X_{ni}\|_{\mathbb{H}}^2 = 1, \quad i = 1, \dots, I.$$

Here, ϵ_n are i.i.d. random variables with mean zero. In addition, for constants $C_1, C_2 > 0$, we assume that $P\{|\epsilon_n| > t\} \leq C_1 \exp(-C_2 t^2)$ for all $t \geq 0$ and $n \in \{1, 2, \dots, N\}$.

The sub-Gaussian tail condition on the errors is satisfied, for instance, by Gaussian random variables; see Section 2.3 of Boucheron et al. (2013).

An important consideration is that the number of predictors I and the number of active predictors I_0 are not fixed but depend on the sample size N . I_0 is assumed to be relatively small compared to both the sample size and the total number of predictors, whereas I is allowed to grow exponentially with the sample size.

The setting introduced here is very general, and several special cases can be retrieved. For example, if we assume $\mathbb{H} = L^2[0, 1]$, the model finds the following famous form

$$Y_n = \sum_{i=1}^I \int \beta_i^*(t) X_{ni}(t) dt + \epsilon_n.$$

Another special case is $\mathbb{H} = \mathbb{R}$ with the standard inner product. In this case, we retrieve the classic multiple regression model. Other important examples are when \mathbb{H} is an RKHS or a Sobolev space. If $\mathbb{H} = \mathbb{H}_2^1[0, 1]$, i.e., the Sobolev space of real-valued functions over the unit interval with one square-integrable derivative, then

$$Y_n = \sum_{i=1}^I \left(\int_0^1 \beta_i^*(t) X_{ni}(t) dt + \int_0^1 \beta_i^{*'}(t) X_{ni}'(t) dt \right) + \epsilon_n.$$

2.2 Finite-dimensional approximation

In infinite-dimensional Hilbert spaces, the covariance operator is typically non-invertible due to its finite rank. To address this limitation, we consider restricting covariance operators to finite-dimensional subspaces of \mathbb{K} . Following the approach in Fan et al. (2015), we consider a given sequence of integers $m = m_N = o(N)$, which depends solely on the sample size N . Let $\mathbb{K}^{(m)}$ denote the m -dimensional subspace of \mathbb{K} spanned by $\{v_1, \dots, v_m\}$, with $\mathbb{K}^{(m)\perp}$ representing its orthogonal complement. The projections of β_i on $\mathbb{K}^{(m)}$ and $\mathbb{K}^{(m)\perp}$ are denoted by $\beta_i^{(m)}$ and $\beta_i^{(m)\perp}$, respectively. Analogous notation is used for the projections of X_{ni} onto $\mathbb{H}^{(m)}$ and $\mathbb{H}^{(m)\perp}$.

We aim to approximate the functional coefficients and predictors while ensuring that approximation errors remain controlled. For this reason, we impose standard assumptions on their bounds.

Assumption 2. $I_0 = O(m)$, and there exist constants $b_1, b_2 > 0$ and $\gamma > 1$ such that the active coefficient and predictor functions satisfy:

$$\|\beta_i^*\|_{\mathbb{K}} \leq b_1 \quad \text{and} \quad \sup_{1 \leq n \leq N} \theta_l \langle X_{ni}, v_l \rangle_{\mathbb{H}}^2 \leq b_2 l^{-\gamma} \quad \text{for all } i = 1, \dots, I_0 \text{ and } l > 1.$$

The first condition implies that the true coefficients are uniformly bounded, a standard assumption in infinite-dimensional regression models (Fan et al., 2015). The second condition is satisfied, for example, when $\|X^{[i]}\|_{\mathbb{H}}$, the column of the design matrix related to i^{th} predictor, is uniformly bounded and the operator K exhibits a polynomial decay rate: $\theta_l \leq Cl^{-\gamma}$ for some constants $C > 0$ and $\gamma > 1$. All kernels considered in this paper exhibit polynomial decay rates of the form $\theta_l \leq Cl^{-(1+2\nu)}$ (Widom, 1964). Thus, for any smoothing parameter $\nu > 0$, the required decay rate assumption on K is satisfied. Consequently, Assumption 2 holds whenever we have a bounded design. A similar condition is used in Roche (2023), where a deterministic design matrix is considered.

The expansions of the predictors and the coefficients are given by

$$X_{ni} = \sum_{l=1}^{+\infty} \langle X_{ni}, v_l \rangle_{\mathbb{H}} v_l, \quad \beta_i^* = \sum_{l=1}^{+\infty} \langle \beta_i^*, v_l \rangle_{\mathbb{H}} v_l.$$

If we restrict the predictors and coefficients to the m -dimensional subspaces, we obtain the following approximation:

$$Y_n = \sum_{i=1}^{I_0} \left\langle \beta_i^{*(m)}, X_{ni}^{(m)} \right\rangle_{\mathbb{H}} + \sum_{i=1}^{I_0} e_{ni} + \epsilon_n, \quad (6)$$

where e_{ni} denotes the approximation error, defined as $e_{ni} = \sum_{l=m+1}^{\infty} \langle X_{ni}, v_l \rangle_{\mathbb{H}} \langle \beta_i^*, v_l \rangle_{\mathbb{H}}$. In Proposition 2 of Appendix A.2, we show that, under Assumption 2, the approximation errors converge uniformly to zero as $m \rightarrow +\infty$. This allows us to consider the following finite-dimensional truncation of the model (5):

$$Y_n = \sum_{i=1}^{I_0} \left\langle \beta_i^{*(m)}, X_{ni}^{(m)} \right\rangle_{\mathbb{H}} + \epsilon_n. \quad (7)$$

To estimate the finite-dimensional coefficients, we consider the objective function of SOFIA:

$$L_{\lambda} : \mathbb{K}^{(m)} \longrightarrow \mathbb{R}^+, \quad L_{\lambda}(\beta) = \frac{1}{2N} \sum_{n=1}^N \left(Y_n - \sum_{i=1}^I \left\langle \beta_i, X_{ni}^{(m)} \right\rangle_{\mathbb{H}} \right)^2 + \lambda \sum_{i=1}^I \tilde{w}_i \|\beta_i\|_{\mathbb{K}}. \quad (8)$$

The weights \tilde{w}_i are chosen adaptively. Initially, all weights are set to 1 to obtain a preliminary estimate $\tilde{\beta}_i$. In the subsequent adaptive step, the weights are updated as $\tilde{w}_i = 1/\|\tilde{\beta}_i\|_{\mathbb{K}}$.

Next, we introduce some proper notation that will be used in the sequel. We use bold symbols to denote vectors and matrices. Let $\mathbf{X} = (X_{nj}) \in \mathbb{H}^{N \times I}$ be the Hilbert-valued deterministic design matrix, which we partition as $\mathbf{X} = (\mathbf{X}_1, \mathbf{X}_2)$, where $\mathbf{X}_1 \in \mathbb{H}^{N \times I_0}$ and $\mathbf{X}_2 \in \mathbb{H}^{N \times (I - I_0)}$ represent the submatrices of active and null predictors, respectively. We use $\mathbf{X}^{[i]}$ to denote the i^{th} column of \mathbf{X} , which is a vector in \mathbb{H}^N . The support of β^* is thus defined as $\mathcal{S} = \{1, \dots, I_0\}$ and its complement is denoted by \mathcal{S}^c . When there is no ambiguity, we will denote the inner product and norm of both \mathbb{K}^I and \mathbb{K} using the same notation.

Since the least squares estimator is based on the inner product of \mathbb{K} , we have to define the covariance operator between two predictors as an operator on \mathbb{K} . For $i, j = 1, \dots, I_0$, the empirical covariance operators are defined as

$$\hat{\Gamma}_{ij} : \mathbb{K} \rightarrow \mathbb{K}, \quad \hat{\Gamma}_{ij}(h) = \frac{1}{N} \sum_{n=1}^N \langle h, K(X_{nj}) \rangle_{\mathbb{K}} K(X_{ni}). \quad (9)$$

These operators incorporate the projection of predictors in the range of K . In addition, we define the Hilbert-valued cross-covariance for $i = 1, \dots, I_0$ as

$$\hat{\Gamma}_{YX_i} = \frac{1}{N} \sum_{n=1}^N Y_n K(X_{ni}) \in \mathbb{K}.$$

We denote by $\hat{\Gamma}_{X_1}$ the $I_0 \times I_0$ matrix of operators $\hat{\Gamma}_{ij}$ and define the vector of cross-covariance operators as $\hat{\Gamma}_{YX_1} = (\hat{\Gamma}_{YX_1}, \dots, \hat{\Gamma}_{YX_{I_0}})^\top$. The cross-covariance operator-valued matrix between null and active predictors is denoted by $\hat{\Gamma}_{X_2X_1}$ and is defined analogously.

We use the superscript (m) for the finite-dimensional counterparts. For instance, for $i, j = 1, \dots, I$, the finite-dimensional covariance operators are

$$\hat{\Gamma}_{ij}^{(m)} : \mathbb{K}^{(m)} \rightarrow \mathbb{K}^{(m)}, \quad \hat{\Gamma}_{ij}^{(m)}(h) = \frac{1}{N} \sum_{n=1}^N \langle h, K(X_{nj}^{(m)}) \rangle_{\mathbb{K}} K(X_{ni}^{(m)}).$$

In the context of scalar-on-function regression models, the definitions of the oracle estimator and the oracle property differ slightly. In what follows, we first define the oracle estimator and then recall the precise formulation of the oracle property.

Typically, the oracle estimator, denoted by $\hat{\beta}^O = (\hat{\beta}_1^O, \dots, \hat{\beta}_I^O)$, is defined as the least squares estimator for the active predictors, while it is set to zero for the inactive ones. However, in scalar-on-function regression, the empirical covariance matrix $\hat{\Gamma}_{X_1}$ is always singular, making the least squares estimator potentially biased. Consequently, the oracle estimator must be defined on finite-dimensional subspaces to ensure well-posedness. Furthermore, as noted in Parodi and Reimherr (2018), when the coefficient functions are assumed to belong to the subspace \mathbb{K} , the oracle estimator is no longer the classical least squares estimator in \mathbb{H} . Instead, it must be constructed using projections onto \mathbb{K} . Since only the first I_0 predictors are assumed to be significant, the oracle estimator is computed by only these predictors. More precisely, it is obtained by minimizing the least squares estimator for $\beta_i \in \mathbb{K}^{(m)}$ for $i = 1, \dots, I_0$:

$$\hat{\beta}^{O(m)} = \arg \min_{\beta_1, \dots, \beta_{I_0} \in \mathbb{K}^{(m)}} \frac{1}{2N} \sum_{n=1}^N \left(Y_n - \sum_{i=1}^{I_0} \langle \beta_i, K(X_{ni}^{(m)}) \rangle_{\mathbb{K}} \right)^2.$$

To find the minimizer, for each $i = 1, \dots, I_0$, we set the functional derivative with respect to β_i to zero.

$$\frac{\partial}{\partial \beta_i} \left(\frac{1}{2N} \sum_{n=1}^N \left(Y_n - \sum_{j=1}^{I_0} \langle \beta_j, K(X_{nj}^{(m)}) \rangle_{\mathbb{K}} \right)^2 \right) = 0.$$

This yields to the equations

$$\sum_{n=1}^N K(X_{ni}) \left(Y_n - \sum_{j=1}^{I_0} \langle \hat{\beta}_j^{O(m)}, K(X_{nj}^{(m)}) \rangle_{\mathbb{K}} \right) = 0, \quad i = 1, \dots, I_0.$$

Using the notation (9), we can write the oracle estimator in the matrix form

$$\hat{\beta}_1^{O(m)} = \hat{\Gamma}_{X_1}^{(m)-1} \hat{\Gamma}_{Y X_1}^{(m)}.$$

An important fact to note is that while the Lasso estimator is not necessarily unique, the oracle estimator is unique because it is the minimizer of a strictly convex objective function. One of our key results is that the SOFIA estimator converges to the oracle estimator as the sample size (and consequently the dimension of the underlying space) increases.

Next, we turn to the definition of the oracle property in the functional context. For classic regression, this is usually expressed as having asymptotically normal estimates and estimating the true support with probability tending to one (Fan and Li, 2001; Zou, 2006). For functional data, when the predictors are scalars, the normality is replaced by a more direct assumption that an estimator is asymptotically equivalent to the oracle estimator. The definition of the oracle estimator for function-on-scalar regression models is given in Definition 3 of Fan and Reimherr (2017). According to the latter, an estimate $\hat{\beta}$ of β^* satisfies the functional oracle property if

$$P\left(\hat{\beta} \stackrel{S}{=} \beta^*\right) \rightarrow 1 \quad \text{and} \quad \sqrt{N} \left\| \hat{\beta} - \hat{\beta}^O \right\|_{\mathbb{K}} = o_P(1)$$

when $N \rightarrow +\infty$. Here, $\stackrel{S}{=}$ indicates that $\hat{\beta}$ and β^* have the same support, and $\hat{\beta}^O$ is the least square estimator on the active predictors and zero for the null ones.

When predictors are functions, the infinite-dimensional least squares estimator is not necessarily unbiased. Therefore, it is natural to consider the oracle estimator as a sequence of estimators defined on nested finite-dimensional subspaces. Therefore, in our framework, we define the functional oracle property as follows.

Definition 1. *An estimate $\hat{\beta}^{(m)}$ of β^* is said to satisfy the functional oracle property if*

$$P\left(\hat{\beta}^{(m)} \stackrel{S^{(m)}}{=} \beta^{*(m)}\right) \rightarrow 1 \quad \text{and} \quad \sqrt{N} \left\| \hat{\beta}^{(m)} - \hat{\beta}^{O(m)} \right\|_{\mathbb{K}} = o_P(1)$$

when $N \rightarrow +\infty$.

2.3 Restricted eigenvalue condition

In our approach, as a first step, we set all the weights in the objective function (8) to be 1. However, the obtained estimator is far from achieving the oracle property, as is known even in the scalar case (Fan and Li, 2001). Nevertheless, in Theorem 1, we show that under an appropriate version of the RE condition, a tight bound for the distance between the true and the estimated coefficients can be found. This bound will be used in the adaptive step to prove the oracle property.

When the predictors are functional, the classic definition of the RE condition is never met. This is because when the dimension of the underlying space is infinity, the lower bound in the RE condition is always zero (Roche, 2023, Lemma 2.1). To overcome this issue, Roche (2023) proposed defining RE as a sequence $\alpha_N^{(m)}$ of positive (possibly zero) values. We adopt this approach with some key modifications and consider the following condition.

Assumption 3. (RE condition) *For the dimension m , there exists a positive number α_m such that*

$$\alpha_m := \min \left\{ \frac{\left\| \Gamma_{XX}^{(m)1/2} \delta \right\|_{\mathbb{K}}}{\left\| \delta \right\|_{\mathbb{K}}} : |J| \leq I_0, \delta = (\delta_1, \dots, \delta_p) \in \mathbb{K}^{(m)} \setminus \{0\}, \left\| \delta_{J^c} \right\|_{\ell_1/\mathbb{K}} \leq 3 \left\| \delta_J \right\|_{\ell_1/\mathbb{K}} \right\},$$

where $\|\boldsymbol{\delta}\|_{\mathbb{K}} = \left(\sum_{i=1}^p \|\delta_i\|_{\mathbb{K}}^2\right)^{1/2}$ represents the ℓ_2 norm, $\|\boldsymbol{\delta}_J\|_{\ell_1/\mathbb{K}} = \sum_{i \in J} \|\delta_i\|_{\mathbb{K}}$ and J^c denotes the complement of the set J .

Our RE condition differs from that of Roche (2023) in two key aspects. First, in our definition, the covariance operators are constructed using the approximated predictors instead of the predictors. Second, the dimension is assumed to depend on the sample size and must always be smaller than that. Indeed, in Roche (2023), the dimension m and the sample size N are treated as independent, allowing m to grow to infinity while N remains fixed. In this setting, for sufficiently large dimensions, $\alpha_N^{(m)}$ can become zero, which is problematic for our theoretical analysis. In contrast, in our setting m depends on N , and $m = O(N)$. In this way, the lower bounds $\alpha^{(m)}$ in 3 can form a sequence of positive non-zero scalars, typically tending to zero. For more details on the RE condition, see Bickel et al. (2009) for Lasso, Lounici et al. (2011) for group Lasso, Bellec and Tsybakov (2017) for a general convex penalty, and Barber et al. (2017) for function-on-scalar models.

2.4 Asymptotic assumptions

The following technical assumptions will be used to analyze the asymptotic behavior of our model. Such assumptions are well known in the literature. However, if the design matrix is scalar-valued, the upper and lower bounds are typically assumed to be constant: see Huang et al. (2008); Fan and Reimherr (2017); Parodi and Reimherr (2018); Mirshani and Reimherr (2021). Following Roche (2023), we assume that these bounds are sequences that tend to zero as m increases. **wE STUDY** The relation between the RE condition and Assumption 4 in Proposition 3 in Appendix B. Specifically, we show that when the covariance between null predictors tends to zero rapidly, the RE condition is met under Assumption 4.

Assumption 4. *For the dimension m , the following conditions hold.*

1. Let σ_{\min} and σ_{\max} be the smallest and largest eigenvalues of $\hat{\Gamma}_{X_1}^{(m)}$, respectively. There exists $\tau_m > 0$ such that

$$\frac{1}{\tau_m} \leq \sigma_{\min} \left(\hat{\Gamma}_{X_1}^{(m)} \right) \leq \sigma_{\max} \left(\hat{\Gamma}_{X_1}^{(m)} \right) \leq \tau_m.$$

2. Let $b_m = \min_{i=1, \dots, I_0} \|\beta_i^{*(m)}\|_{\mathbb{K}}$. Then, $b_m^2 \gg \tau_m^2 I_0^2 \log(I) / \alpha_m^4 N$.

3. The tuning parameter λ satisfies the bounds

$$\frac{I_0^3 \log(I)}{\alpha_m^4 N} \ll \lambda \ll \frac{b_m}{\tau_m \sqrt{I_0 N}}.$$

4. Let $\|\cdot\|_{op}$ denote the operator norm. Then, $\|\hat{\Gamma}_{X_2 X_1}^{(m)} \hat{\Gamma}_{X_1}^{(m)-1}\|_{op} = \varphi_m < 1$.

The four listed conditions are counterparts to some standard assumptions in the high-dimensional regression literature. The first, often called the ‘‘design matrix condition’’, ensures that the true predictors exhibit regular behavior and are not excessively correlated. This condition is imposed by setting fixed lower and upper bounds for the eigenvalues. In our approach, since $\hat{\Gamma}_{X_1}$ is a finite-rank operator on an infinite-dimensional Hilbert space \mathbb{H}^{I_0} , it is never injective, and so 0 is always an eigenvalue. To address this, we restrict our analysis to finite-dimensional subspaces of the underlying infinite-dimensional space, making it natural to impose a sequence of bounds that

depend on both the dimension and the sample size. Typically, $(\tau_m)^{-1}$ has zero as an accumulation point, since, as the sample size increases, $\hat{\Gamma}_{X_1}^{(m)}$ converges to a compact operator (not necessarily of finite rank), and compact operators always have 0 as a limit point of their eigenvalues. This implies that the design matrix becomes increasingly ill-conditioned and nearly singular as the sample size grows. This ill-posedness is controlled by assumptions on the minimum norm of the coefficients and the tuning parameter.

The second condition, known as the “minimum signal condition”, allows the smallest β_i^* to vary with the sample size, the dimension, and the lower bound of the eigenvalues while ensuring that it does not become too small. If $(\tau_m)^{-1}$ decays too rapidly in relation to sample size, number of predictors and number of active predictors, then there is no guarantee that the model will be able to select predictors with small norms.

The third prevents the tuning parameter from growing too rapidly or too slowly. The lower bound prevents overfitting by controlling false positives, while the upper bound ensures that relevant predictors are not excessively penalized, avoiding false negatives.

The last condition, known as the “irrepresentable condition”, ensures that the true and the null predictors do not exhibit a high correlation. In the literature on scalar predictors, the sequence φ_m is supposed to be a fixed number, usually less than 1. This condition has been established as a necessary condition for having the oracle property: see, for example, Zhao and Yu (2006) for formal definitions and proofs.

3 Theoretical results

This section presents the theoretical results of the paper. We begin with a concentration inequality that bounds the tail probability of a weighted sum of Hilbert space-valued random variables. The lemma extends Lemma 1 in the supplementary material of Huang et al. (2008) to the Hilbert space setting and serves as a key component in the proofs of Theorems 1 and 2. The proof is given in Appendix A.3.

Lemma 1 (Hilbert-Valued Concentration Inequality). *Let $\mathbf{X} = (X_1, \dots, X_N)$ be a vector in a separable Hilbert space \mathbb{H} with $N^{-1}\|\mathbf{X}\|_{\ell_2/\mathbb{H}} = 1$, and let $\boldsymbol{\epsilon} = (\epsilon_1, \dots, \epsilon_N)$ satisfy Assumption 1. Define $Z := N^{-1} \sum_{n=1}^N \epsilon_n X_n \in \mathbb{H}$. Then, for any $t > 0$,*

$$P(\|Z\|_{\mathbb{H}} > t) \leq \exp\left(-\frac{Nt^2}{M}\right),$$

where $M > 0$ is a constant, depending only on the constants C_1 and C_2 in Assumption 1.

The following theorem provides bounds for the estimation and prediction errors of the unweighted Lasso. A similar theorem for scalar regression can be found in Chapter 6 of Bühlmann and Van De Geer (2011). The function-on-scalar case is proved in Barber et al. (2017). Our contribution in this theorem is two-fold. First, we design a concentration inequality for Hilbert-valued design matrices. Then, we develop the estimation and error analysis in a separable Hilbert space.

The nonasymptotic convergence rates are similar to those of the scalar case. This is because we prove that the Hilbert-valued concentration inequality mirrors the scalar structure (see Appendix A.3 for the proof). However, the asymptotic behavior crucially depends on the sequence $\{\alpha_m\}_{m \in \mathbb{N}}$. This sequence is supposed to be fixed in classic regression models, so it does not have any impact when the sample size increases. However, in the presence of functional predictors, this

sequence always tends to zero and its behavior significantly affects the convergence rate of the estimator. The proof of this theorem is provided in Appendix A.4.

Theorem 1. *Let Assumptions 1, 2 and 3 hold. Let $\tilde{\beta}^{(m)}$ be any minimizer of the Lasso estimator (8) with weights equal to 1. Let $\delta \in (0, 1)$ and $\lambda \geq \sqrt{N^{-1}M \log(I/\delta)}$, where $M > 0$ is the constant in Lemma 1. Then,*

$$P \left(\left\| \Gamma_{XX}^{(m)1/2} \left(\tilde{\beta}^{(m)} - \beta^{*(m)} \right) \right\|_{\mathbb{K}} \leq \frac{4\lambda\sqrt{I_0}}{\alpha_m} \right) \geq 1 - \delta$$

and

$$P \left(\left\| \tilde{\beta}^{(m)} - \beta^{*(m)} \right\|_{\ell_1/\mathbb{K}} \leq \frac{8\lambda I_0}{\alpha_m^2} \right) \geq 1 - \delta.$$

The following corollary is a direct result of Theorem 1, which makes (unweighted) Lasso a very good starting point for the adaptive model. In this corollary, the upper bounds are selected in a way that is consistent with the literature (Lounici et al., 2011; Barber et al., 2017; Fan and Reimherr, 2017; Parodi and Reimherr, 2018).

Corollary 1. *Let Assumptions 1, 2 and 3 hold, and λ decay with rate $\lambda \sim \sqrt{\log(I)/N}$. Then, for any minimizer $\tilde{\beta}^{(m)}$ of the function (8) with weights equal to 1, when $N \rightarrow +\infty$,*

$$\sup_{j \in \mathcal{S}} \left\| \tilde{\beta}_j^{(m)} - \beta_j^{*(m)} \right\|_{\mathbb{K}} = O_p(\sqrt{r_N}) \quad \text{with} \quad r_N := \frac{I_0^2 \log I}{\alpha_m^4 N}.$$

We are now in a position to state our main result. We show that, when the sample size grows, with probability tending to 1, SOFIA selects the true predictors and converges to the oracle estimator. See Appendix A.6 for the proof.

Theorem 2 (Functional Oracle Property). *For $i = 1, \dots, I$ let $\tilde{\beta}_i^{(m)}$ be the estimator of Theorem 1 and $\hat{\beta}_i^{(m)}$ a minimizer of function (8) with weights $\tilde{w}_i = \|\tilde{\beta}_i^{(m)}\|_{\mathbb{K}}^{-1}$.*

(i) *If Assumptions 1, 2 and 4 hold, then, when $N \rightarrow +\infty$,*

$$P \left(\hat{\beta}^{(m)} \stackrel{s}{=} \beta^{*(m)} \right) \rightarrow 1.$$

(ii) *If, in addition, $\lambda \ll b_m \tau_m / \sqrt{I_0 N}$, then, when $N \rightarrow +\infty$,*

$$\sqrt{N} \left\| \hat{\beta}^{(m)} - \hat{\beta}^{O(m)} \right\|_{\mathbb{K}} = o_P(1).$$

(iii) *If, in addition, $\|\beta_i^{*(m)\perp}\|_{\mathbb{K}} = o_p(1/\sqrt{I_0 N})$ for all $i \in \mathcal{S}$, then, when $N \rightarrow +\infty$,*

$$\sqrt{N} \left\| \hat{\beta}^{(m)} - \beta^* \right\|_{\mathbb{K}} = o_P(1).$$

The first part of the theorem establishes that SOFIA recovers the true support with probability tending to one. This guarantees consistent variable selection in the high-dimensional functional setting. The second part shows that SOFIA is equivalent to the oracle estimator on the finite-dimensional space $\mathbb{K}^{(m)}$. As mentioned in Definition 1, this means that SOFIA is asymptotically equivalent to the oracle estimator. The third part claims that if the tail of the projections of β_i^* in $\mathbb{K}^{(m)}$ decays sufficiently fast, then the finite-dimensional Lasso estimator converges to β^* in the

strong topology of \mathbb{K} . As a result, SOFIA achieves full consistency in \mathbb{K} despite operating through finite-dimensional approximations.

The proof of Theorem 2 is inspired by the proofs in Huang et al. (2008) and Parodi and Reimherr (2018). It extends a concentration inequality for sub-Gaussian variables to the case of random elements in separable Hilbert spaces. Furthermore, we derive the oracle property by controlling both estimation and approximation errors, which are delicately balanced by using spectral properties of the compact operator defining the Hilbert space. This requires careful handling of operator-valued covariance structures in infinite-dimensional spaces.

4 Implementation

To implement SOFIA, we revisit the FLAME method in Parodi and Reimherr (2018) and introduce several modifications to account for functional predictors. To find the minimizers of the objective function (8), we propose a coordinate descent algorithm using the functional subgradient. The definitions of the functional subgradient can be found in Chapter 16 of Bauschke et al. (2011). In Appendix A.5, we show that, for $i = 1, \dots, I$ the functional subgradient of the objective function (8) in \mathbb{K} is

$$\begin{aligned} \frac{\partial}{\partial \beta_i} L_\lambda(\boldsymbol{\beta}) &= -\frac{1}{N} \left(\sum_{n=1}^N \left(Y_n - \sum_{j=1}^I \langle \beta_j, K(X_{nj}^{(m)}) \rangle_{\mathbb{K}} \right) K(X_{ni}^{(m)}) \right) \\ &+ \lambda \tilde{w}_i \begin{cases} \|\beta_i\|_{\mathbb{K}}^{-1} \beta_i & \text{if } \beta_i \neq 0, \\ \{h \in \mathbb{K} : \|h\|_{\mathbb{K}} \leq 1\} & \text{if } \beta_i = 0. \end{cases} \end{aligned}$$

To update the i^{th} coordinate, set $\check{\beta}_i = N^{-1} \sum_{n=1}^N (Y_n - \sum_{j \neq i} \langle \hat{\beta}_j, K(X_{nj}^{(m)}) \rangle_{\mathbb{K}}) K(X_{ni}^{(m)})$ and let the other coordinates be fixed. Then, we can separate the contribution of the i^{th} predictor and write

$$\frac{\partial}{\partial \beta_i} L_\lambda(\boldsymbol{\beta}) = -\check{\beta}_i + \hat{\Gamma}_{ii}^{(m)}(\beta_i) + \lambda \tilde{w}_i \begin{cases} \|\beta_i\|_{\mathbb{K}}^{-1} \beta_i & \text{if } \beta_i \neq 0, \\ \{h \in \mathbb{K} : \|h\|_{\mathbb{K}} \leq 1\} & \text{if } \beta_i = 0. \end{cases} \quad (10)$$

Only for the implementation part, we assume that $\hat{\Gamma}_{ii}^{(m)}$ is equal to the identity matrix. This is equivalent to a well-known assumption, called ‘‘group-wise orthonormality condition’’ in the group Lasso (Roche, 2023). This assumption is stronger than Assumption 4 because it directly implies that $\|\hat{\Gamma}_{ii}^{(m)}\| \leq 1$.

We set eq. (10) to zero to find the minimum. Therefore, $\hat{\beta}_i$ will be a minimizer of $L_\lambda(\boldsymbol{\beta})$ if it satisfies the following equation:

$$\hat{\beta}_i = \begin{cases} 0, & \|\check{\beta}_i\|_{\mathbb{K}} \leq \lambda \tilde{w}_i, \\ \left(1 + (\lambda \tilde{w}_i) \|\hat{\beta}_i\|_{\mathbb{K}}^{-1}\right)^{-1} \check{\beta}_i, & \|\check{\beta}_i\|_{\mathbb{K}} > \lambda \tilde{w}_i. \end{cases} \quad (11)$$

The first case in eq. (11) provides an upper bound for λ in the estimation process. If $\lambda \geq (\tilde{w}_i N)^{-1} \|\sum_{n=1}^N Y_n K(X_{ni}^{(m)})\|_{\mathbb{K}}$ for all $i = 1, \dots, I$, all the predictors will be discarded. Therefore, to select the grid of λ , we start with this value and decrease it in logarithmically spaced intervals at a prespecified rate until we reach the desired number of values for λ . The second case in eq. (11)

enables us to update non-zero coefficients. For $\hat{\beta}_i \neq 0$, we have

$$\hat{\beta}_i = \left(1 + \frac{(\lambda \tilde{w}_i)}{\|\hat{\beta}_i\|_{\mathbb{K}}} \right)^{-1} \check{\beta}_i.$$

This equation does not have a closed form, even for the scalar design. The problem is that the norm of $\hat{\beta}_i$ on the right-hand side is unknown. To overcome this issue, we compute the \mathbb{K} -norm and apply Parseval's identity:

$$\|\hat{\beta}_i\|_{\mathbb{K}}^2 = \sum_{l=1}^m \left\langle \left(1 + \frac{\lambda \tilde{w}_i}{\|\hat{\beta}_i\|_{\mathbb{K}}} \right)^{-1} \check{\beta}_i, v_l \right\rangle^2 = \left(1 + \frac{\lambda \tilde{w}_i}{\|\hat{\beta}_i\|_{\mathbb{K}}} \right)^{-2} \sum_{l=1}^m \langle \check{\beta}_i, v_l \rangle^2.$$

After some simplifications, we obtain the equation

$$1 = \frac{\sum_{l=1}^m \langle \check{\beta}_i, v_l \rangle^2}{\left(\|\hat{\beta}_i\|_{\mathbb{K}} + \lambda \tilde{w}_i \right)^2}.$$

We use the NLOPT_LN_COBYLA algorithm from the R package `nloptr` to solve this nonlinear equation for $\|\hat{\beta}_i\|_{\mathbb{K}}$. Then, we use a coordinate descent algorithm to iteratively compute estimates $\beta^{(t)}$ for $t = 1, \dots, T$ that converge to $\hat{\beta}$. The iterative algorithm stops when the improvement in the \mathbb{K} -norm of the estimate of β reaches a pre-specified threshold.

As explained in Section 2, we run the algorithm twice. First, we set all the weights \tilde{w}_i to 1 to obtain an initial estimate of the coefficients. Then, for those that have a non-zero norm, we set $\tilde{w}_i = 1/\|\check{\beta}_i^{(m)}\|_{\mathbb{K}}$ and run the algorithm once again to improve the variable selection and refine the estimation.

The predictors are expanded by the eigenfunctions of the operator K . To determine the number of basis functions, we use the minimum of N and the smallest number of eigenvalues that satisfy $\sum_{j=1}^J \theta_j \geq 0.99 \sum_{j=1}^{\infty} \theta_j$, which mimics the 99% explanation of the data variability in FPCA. As stopping criteria, we use a maximum number of iterations of the nonlinear algorithm, a threshold for the improvement of the estimation error, and a kill switch, which means that the process stops when the number of selected variables exceeds a given number. We employ 5-fold cross-validation to determine the optimal value of λ .

5 Simulation study

In this section, we conduct a comprehensive simulation study to evaluate how SOFIA performs in practice. We consider both the variable selection accuracy and the predictive performance in several scenarios. Specifically, we generate datasets under different model complexities and signal-to-noise ratios, allowing us to compare SOFIA with existing benchmark methods under various conditions.

We take the simulation framework from Gertheiss et al. (2013) and introduce some modifications. We set $\mathbb{H} = L^2[0, 1]$ and the response is generated according to the model

$$Y_n = \sum_{j=1}^{I_0} \int_0^1 \beta_j(t) X_{nj}(t) dt + \epsilon_n.$$

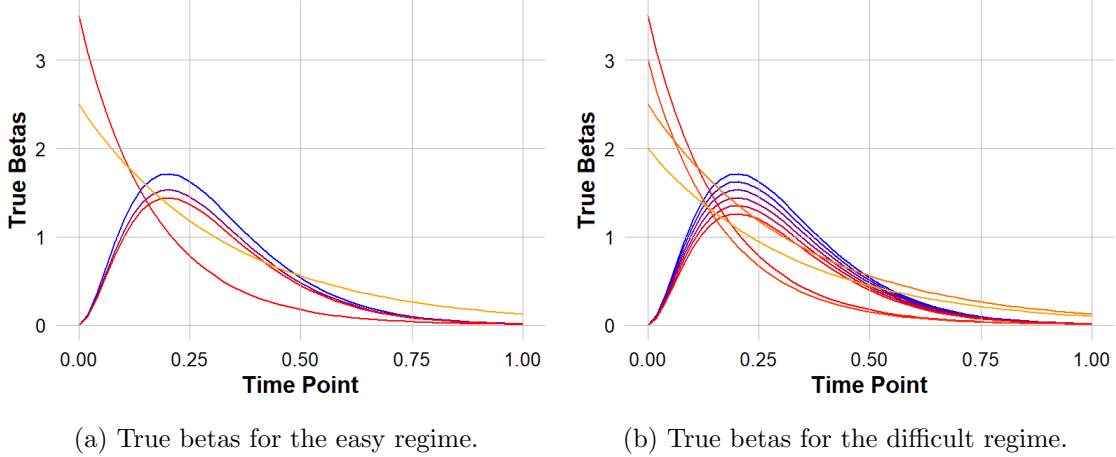


Figure 1: The coefficient functions $\beta(t)$. Some are modeled using Gamma density functions, while others follow exponential density functions.

The functional predictors are defined as

$$X_{nj}(t) = \sum_{r=1}^5 (a_{njr} \sin(2\pi t(5 - a_{njr})) - m_{njr}),$$

where $n = 1, \dots, 500$ denotes the observation index and t takes 50 equidistant values in the interval $[0, 1]$. The number of predictors, indexed by j , varies between the different experimental scenarios that we consider. The coefficients a_{njr} are independently sampled from the uniform distribution $U(0, 5)$, and m_{njr} are drawn independently from the uniform distribution $U(0, 2\pi)$.

Regarding the coefficient functions β , we consider two regimes and two scales. In the **easy** regime, there are five active predictors: three are based on Gamma density functions, and the remaining two follow exponential shapes. In the **difficult** regime, we include ten active predictors: six are derived from Gamma densities and the other four are based on exponential density functions. Figure 1 displays the true coefficient functions in both regimes.

For the number of predictors, we consider **extensive** and **moderate** scales. On the extensive scale, we include 700 functional predictors, which is particularly challenging due to the large number of predictors relative to the sample size ($N < I$). Among the competing methods, only FASStEn (Boschi et al., 2024) can handle this large functional regression setting.

On the moderate scale, the easy regime contains 10 predictors, of which five are active, and the difficult regime contains 30 predictors, of which 10 are active. These moderate-sized settings enable a broader comparison across different model complexities. The evaluation includes five competing methods, and we assess their performance using several criteria that we will detail in the following sections.

For each regime and scale, we consider four levels of signal-to-noise ratio (SNR): $SNR = 0.5, 1, 10, \text{ and } 100$. The noise terms are generated as $\epsilon_n \sim \mathcal{N}(0, \sigma^2)$, where the variance σ^2 is set according to the desired SNR level by the formula $\sigma^2 = \text{var}(\mathbf{Y}^{true})/SNR$. Here the noise-free scalar response is defined as $Y_n^{true} = Y_n - \epsilon_n$, and $\text{var}(\mathbf{Y}^{true})$ denotes its variance over $n = 1, \dots, N$.

For each scenario, the performance of the methods is evaluated on the basis of the average number of true positives and false positives across replications. We assess the prediction accuracy

by computing the root mean squared error (RMSE) on an independently generated test set:

$$\sqrt{\frac{1}{N_{\text{test}}} \sum_{n=1}^{N_{\text{test}}} (Y_n - \hat{Y}_n)^2},$$

with $N_{\text{test}} = 100$. To choose the tuning parameter λ , we examine 100 candidate values using a 5-fold cross-validation.

We assume that K is an integral operator associated with the kernel function $k(t, s)$:

$$(Kf)(t) = \int_0^1 k(t, s)f(s) ds.$$

The space \mathbb{K} corresponds to the RKHS induced by the kernel function $k(t, s)$. In the literature, two kernels are commonly used:

$$k_{\infty}(t, s) = \exp\left(\frac{-|t - s|^2}{\rho}\right), \quad k_{1/2}(t, s) = \exp\left(\frac{-|t - s|}{\rho}\right).$$

The parameter ρ controls the length scale. A lower value of ρ results in a kernel that decays more rapidly as the distance $|t - s|$ increases, leading to functions that exhibit more rapid variations over short distances. The first kernel, known as the Gaussian kernel, is infinitely differentiable and is, therefore, well suited for modeling very smooth data. The second kernel, referred to as the exponential or Laplacian kernel, possesses only one continuous derivative, making it more appropriate for modeling rough data. These kernels belong to a broader class known as Matérn kernels, defined by

$$k_{\nu}(t, s) = \frac{2^{1-\nu}}{\Gamma(\nu)} \left(\frac{\sqrt{2\nu}|t - s|}{\rho}\right)^{\nu} K_{\nu}\left(\frac{\sqrt{2\nu}|t - s|}{\rho}\right),$$

where Γ is the Gamma function and K_{ν} denotes the modified Bessel function of the second kind (Genton, 2001). In addition to the two aforementioned cases, we will consider the Matérn kernel with $\nu = 5/2$ and $\nu = 3/2$ to compare the performance of different levels of smoothness. As ν increases, the eigenvalues of the corresponding kernel decay at a faster rate, ultimately reaching an exponential decay rate as $\nu \rightarrow \infty$, which corresponds to the Gaussian kernel.

5.1 Extensive scale

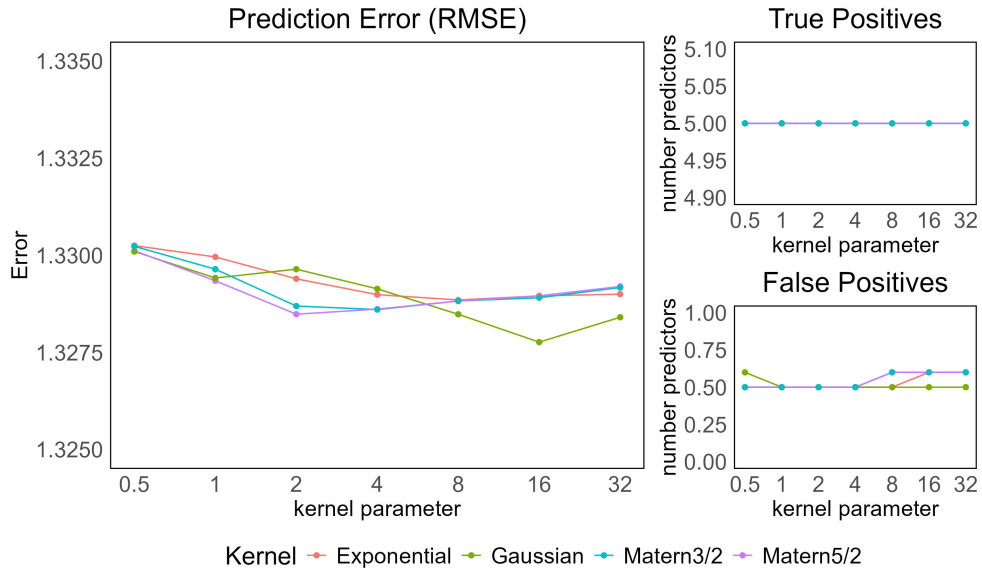
In this high-dimensional setting, we consider 700 predictors with both easy and difficult regimes, as previously described. We evaluate 100 candidate values of λ , spaced logarithmically with a ratio of 0.01, as explained in Section 4. For the kill switch, we set the maximum number of selected predictors to $2I_0$ in each regime.

We begin by comparing the performance of different kernel functions to highlight the impact of kernel choice and parameter settings on variable selection and estimation accuracy. Figures 2 and 3 display the performance of four kernel functions—exponential, Gaussian, Matérn 3/2, and Matérn 5/2—evaluated across a range of parameter values under SNR levels 1 and 10, respectively. The results for the high-noise case (SNR = 0.5) and the near noise-free case (SNR = 100) are presented in Appendix C (Figures 5 and 6). Each figure presents two simulation regimes—easy and difficult—to evaluate the robustness of the method across varying levels of signal strength and predictor complexity.

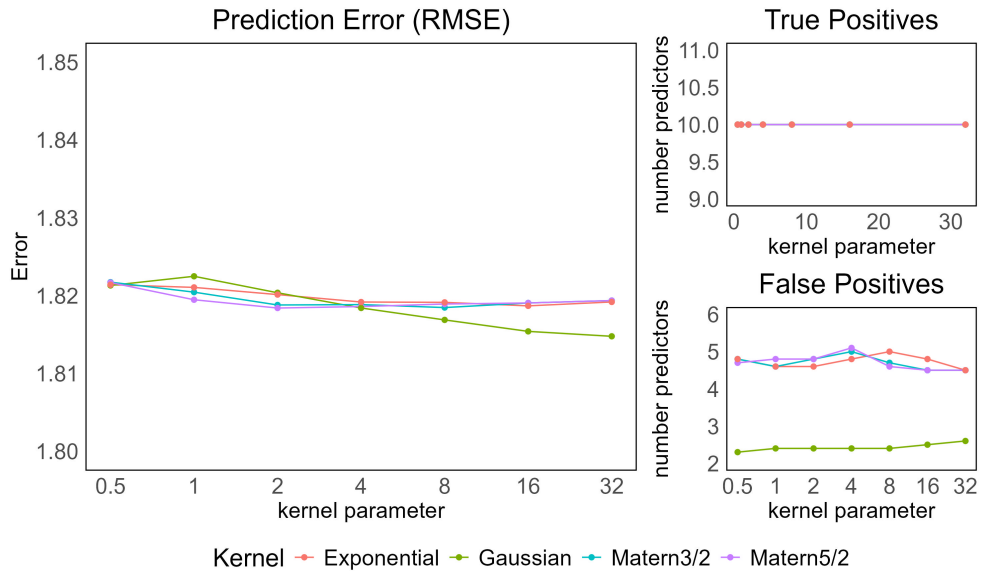
Three performance metrics are used in each scenario: the true positive rate (TP), measuring the number of correctly identified active predictors; the false positive rate (FP), indicating erroneous inclusion of inactive predictors; and the root mean squared error (RMSE), which quantifies prediction accuracy on an independent test set.

Across all kernels and parameters, SOFIA consistently recovers all of the true predictors in both regimes. However, as noise increases, the number of false positives rises, particularly in the difficult regime, where active predictors are harder to distinguish. While all kernels show comparable performance across parameter settings, the Gaussian kernel generally yields fewer false positives in noisier settings, suggesting greater robustness in high-noise environments. By Figure 3 (SNR = 10), all performance metrics show marked improvement, with perfect support recovery and low RMSE—especially in the easy regime—highlighting SOFIA’s capacity to leverage strong signal conditions effectively.

SNR = 1



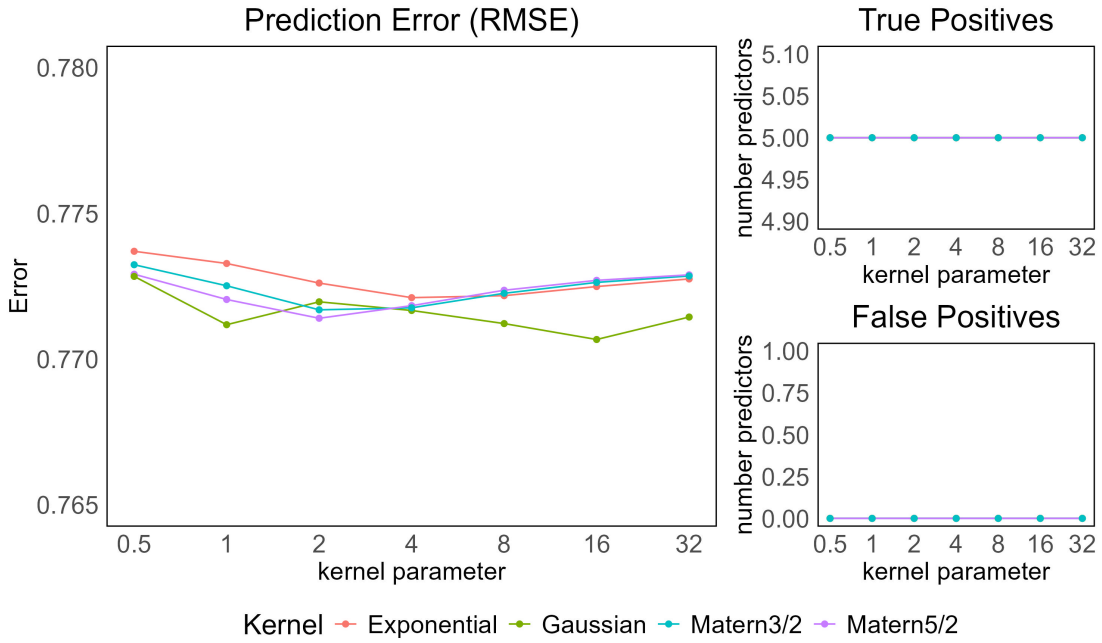
(a) Easy regime



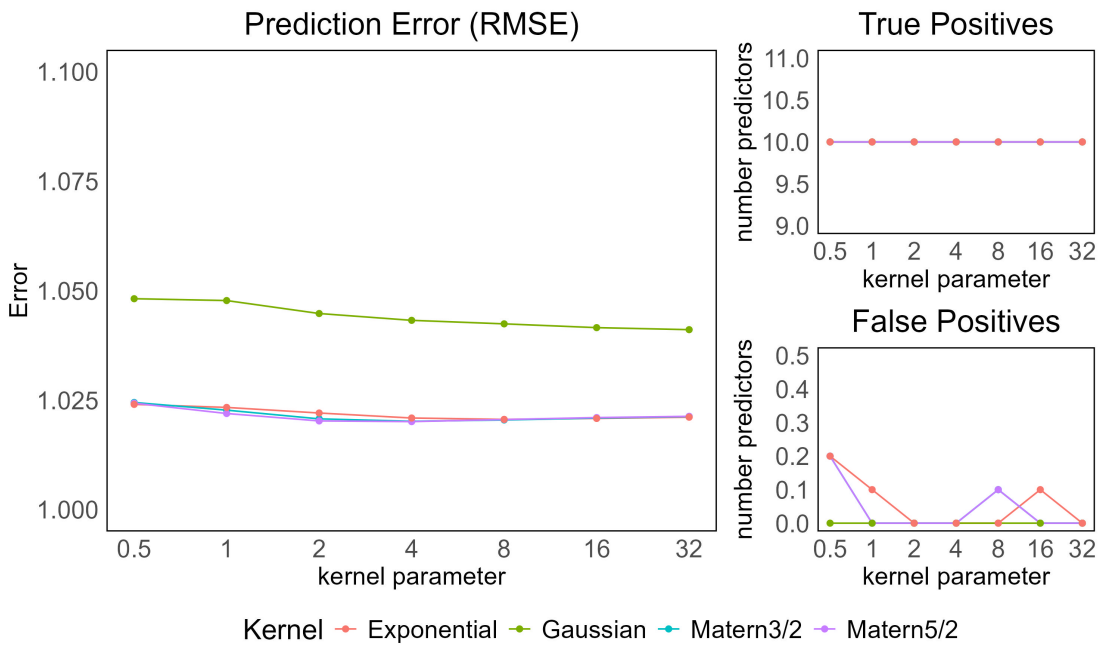
(b) Difficult regime

Figure 2: Comparison of the performance of different kernels under varying parameter values for SNR = 1. Each subfigure shows the true positive rate (TP), false positive rate (FP), and root mean squared error (RMSE) in one regime.

SNR = 10



(a) Easy regime



(b) Difficult regime

Figure 3: Comparison of the performance of different kernels under varying parameter values for SNR = 10. Each subfigure shows the true positive rate, false positive rate, and root mean squared error (RMSE) in one regime.

Table 1 compares the performance of SOFIA and FAStEN by Boschi et al. (2024). We use the Gaussian kernel with parameter $\rho = 8$, which is appropriate for general uses. For both methods, we use $2I_0$ as the kill switch. For all SNR levels, both methods identified all or nearly all true predictors with very few false positives.

In low-SNR settings (SNR = 0.5 and 1), SOFIA achieves lower RMSE than FAStEN, while both methods detect a similar number of true positives. FAStEN shows slightly better control over false positives, particularly in the difficult regime. However, it tends to select fewer true positives. As the SNR increases, SOFIA demonstrates improved support recovery and lower prediction error across all metrics. At high SNR levels (10 and 100), both methods recover all true predictors, but SOFIA consistently achieves lower RMSEs, indicating more accurate coefficient estimation. Overall, SOFIA provides superior predictive performance while maintaining competitive variable selection accuracy.

SNR	Method	Easy ($I_0 = 5$)			Difficult ($I_0 = 10$)		
		TP	FP	RMSE	TP	FP	RMSE
0.5	FAStEN	4.9	0.9	2.22	7.8	2.4	2.87
	SOFIA	4.9	1.7	1.75	10	3.8	2.36
1	FAStEN	5	0.1	1.75	9.6	1.8	2.28
	SOFIA	5	0.5	1.32	10	2.4	1.82
10	FAStEN	5	0	1.21	10	0.1	1.60
	SOFIA	5	0	0.77	10	0	1.04
100	FAStEN	5	0	1.14	10	0	1.52
	SOFIA	5	0	0.69	10	0	0.89

Table 1: Comparison between SOFIA (with a Gaussian kernel, parameter $\rho = 8$) and FAStEN across four SNR levels. Results are computed on a test set of size 100, and they are the average of 10 runs. Bold entries highlight the best-performing method for each metric.

5.2 Moderate scale

Since most existing methods are not computationally feasible for a large number of predictors and cannot handle cases where the number of predictors exceeds the sample size, we reduce the number of predictors to allow for a broader comparison. In this moderate-scale setting, the easy regime includes 10 predictors with five active, while the difficult regime consists of 30 predictors with 10 active. We compare the performance of SOFIA with five other methods: the Standard one of Fan et al. (2015), Adapt1 and Adapt2 of Gertheiss et al. (2013), the one of Roche (2023), and FAStEN of Boschi et al. (2024). To ensure a fair comparison, all methods are run without any kill switch, and we apply each method using its default configuration parameters. We use the Gaussian kernel with the same parameter as in the extensive scale.

Table 2 summarizes the results. In low SNR conditions (SNR = 0.5 and 1), SOFIA and FAStEN effectively balance selection and precision, achieving high true positive rates with relatively low false positives and prediction error. In contrast, Roche does not detect any active predictors under these noisy conditions. Adapt2 performs better than Adapt1 and the Standard method, showing improved selection accuracy, particularly in the difficult regime.

As the SNR increases (SNR = 10 and 100), the performance of all methods improves. SOFIA consistently demonstrates strong stability, achieving low RMSE and high true positive recovery with minimal false positives across both regimes. FASTEN and Roche also show notable gains, particularly in the difficult setting, where they maintain high selection precision with near-zero false positives. Although Standard, Adapt1, and Adapt2 sometimes achieve competitive RMSE at high SNR levels, their elevated false-positive rates make them less suitable for tasks that require precise variable selection.

Overall, when the noise level is moderate to low, all methods recover the true predictors well in the easy regime. However, in the more challenging difficult regime, SOFIA, FASTEN, and Roche demonstrate superior performance in terms of both selection accuracy and robustness.

SNR	Method	Easy ($I_0 = 5$)			Difficult ($I_0 = 10$)		
		TP	FP	RMSE	TP	FP	RMSE
0.5	Standard	5	2.6	1.72	10	11.3	2.50
	Adapt1	5	2.7	1.17	10	11.5	2.28
	Adapt2	5	1	1.73	10	3.6	2.78
	Roche	0	0	2.02	0	0	2.72
	FASTEN	5	0.2	2.3	9.6	1.4	2.95
	SOFIA	5	0	1.95	9.7	0.6	2.28
1	Standard	5	2.3	1.26	10	10.8	1.98
	Adapt1	5	2.5	0.13	10	12.3	0.23
	Adapt2	5	0.7	1.27	10	3.8	2.04
	Roche	0	0	1.65	0	0	2.23
	FASTEN	5	0.2	1.85	10	0.5	2.36
	SOFIA	5	0	1.47	9.9	0	1.72
10	Standard	5	0.6	0.59	10	5.9	1.33
	Adapt1	5	1.1	0.08	10	7.4	0.16
	Adapt2	5	0.2	0.62	10	2.8	1.43
	Roche	5	0	1.04	9.66	0	1.25
	FASTEN	5	0	1.28	10	0.4	1.65
	SOFIA	5	0	0.77	10	0	0.90
100	Standard	5	0.2	0.48	10	3.4	1.24
	Adapt1	5	0.5	0.08	10	5.1	1.50
	Adapt2	5	0.4	0.52	10	2.6	1.35
	Roche	5	0	1.00	10	0	0.57
	FASTEN	5	0	1.20	10	0	1.56
	SOFIA	5	0	0.63	10	0	0.74

Table 2: Comparison between SOFIA (with a Gaussian kernel, parameter $\rho = 8$) and five competitor methods across four SNR levels. Results are computed on a test set of size 100, and they are the average of 10 runs. Bold entries highlight the best-performing method for each metric.

6 Real data analysis

In this section, we apply the SOFIA method to a real-world economic dataset to identify the most relevant functional predictors to forecast GDP growth in Canada. Our goal is twofold: first, to assess the model’s capacity to select meaningful variables in a high-dimensional functional setting, and second, to evaluate the predictive performance of SOFIA compared to classical forecasting methods.

The time-varying nature of economics and finance makes them a relevant area for the FDA. Functional techniques can address many issues in these domains. One challenge is the high frequency of the data, which can lead to overfitting, noise, and computational complexity. FDA offers robust methods to handle and analyze high-frequency data by smoothing and leveraging their continuous nature (Zhang et al., 2023). Another challenge is the heterogeneity of the data time frequencies. Some predictors are reported monthly, while others are reported quarterly or annually (Kapetanios et al., 2016). In the FDA, different frequencies are easily managed because all variables are transformed into curves on a continuous domain and evaluated on a unified frequency scale.

Accurate prediction of GDP growth is crucial for macroeconomic analysis, helping policymakers, financial institutions, and businesses in decision-making and planning. We are interested in cases where multiple macroeconomic predictors are observed, and we want to determine significant variables in GDP growth prediction. We use a dataset from Fortin-Gagnon et al. (2022), which provides a comprehensive macroeconomic database on Canadian economic indicators. We consider a balanced version of the data in the paper that overcomes the issues related to stationarity, missing data, and discontinuities in time series data due to changes in data collection methods or classifications. For our analysis, we use a monthly frequency from January 1981 to December 2019, resulting in a total of 468 months. This time frame excludes the unpredictable COVID-19 pandemic outbreak.

The dataset includes many international, national, and provincial economic variables. To ensure meaningful and interpretable results, we restrict our analysis to national-level indicators and select 20 predictors commonly used in GDP prediction studies. These variables represent various financial sectors and include predictors such as total GDP (`GDP_new`), industrial production GDP (`IP_new`), retail trade GDP (`RT_new`), public administration GDP (`PA_new`), oil production (`OIL_CAN_new`), employment rate (`EMP_CAN`), unemployment rate (`UNEMP_CAN`), new housing price index (`NHOUSE_P_CAN`), housing starts units (`Hstart_CAN_new`), total building permits (`build.Total_CAN_new`), M3 money supply (`M3`), household credit (`CRED_HOUS`), business credit (`CRED_BUS`), bank rate (`BANK_RATE_L`), three-month Treasury bill rate (`TBILL_3M`), total Canada’s official international reserves (`RES_TOT`), total imports (`Imp_BP_new`), total exports (`Exp_BP_new`), exchange rate between the US and the Canadian dollar (`USDCAD_new`), and the inflation rate measured by the Consumer Price Index (`CPI_ALL_CAN`). For complete definitions of the variables, see Fortin-Gagnon et al. (2022).

We construct functional predictors using monthly data by grouping 12 consecutive values without applying additional smoothing, so that the functional representation preserves the original structure of the data. To generate a sufficient number of functional observations, we employ a rolling window method with a one-month shift. Precisely, each functional observation corresponds to a sequence of 12 consecutive months: the first observation consists of a curve obtained by the data from months 1 to 12, the second from months 2 to 13, and so on. Following this procedure, we obtain a functional dataset that contains $n = 456$ observations and $I = 20$ predictors.

For the scalar response, we consider the GDP growth of the month immediately following the

12-month predictors. GDP growth is measured as the change in GDP from one month to the next, using the difference of logarithmic values. This transformed variable is called `GDP_new` in the dataset of Fortin-Gagnon et al. (2022).

Since the data are not smoothed, we employ an exponential kernel with a parameter of 2, which is well-suited for handling rough data and exhibits increased robustness to noise. Given the time-dependent nature of the data, regular cross-validation methods are not applicable. Therefore, we implement a rolling-window cross-validation approach. Specifically, the first 75% of the dataset is used as the initial training set, and the next 5% is used as the test set. In each subsequent fold, we shift both the training and test sets forward by 5% of the total dataset size, ensuring a progressive reallocation of observations. This procedure results in a 5-fold rolling-window cross-validation framework. For the selection of λ , we use a grid of 100 candidate values with a ratio of 0.1.

The predictors selected by SOFIA are total GDP (`GDP_new`), employment rate (`EMP_CAN`) and unemployment rate (`UNEMP_CAN`). Figure 4 presents the estimated β coefficients corresponding to the selected predictors over time. The estimated coefficient functions reveal that `GDP_new` and `EMP_CAN` have a positive relationship with current GDP, with their effects growing stronger over time until the 10th month, suggesting that, in GDP growth forecasting, the growth rate observed three months before has the highest predictive power relative to the other months. In contrast, `UNEMP_CAN` shows a negative effect, indicating that higher unemployment is associated with lower GDP growth. A similar trend around the last three months before can also be seen for this predictor. Interestingly, at the beginning of the time period, all three predictors show a pattern opposite to what is observed later on. This may suggest a form of mean reversion, where early movements are gradually offset or reversed as the economy adjusts over time.

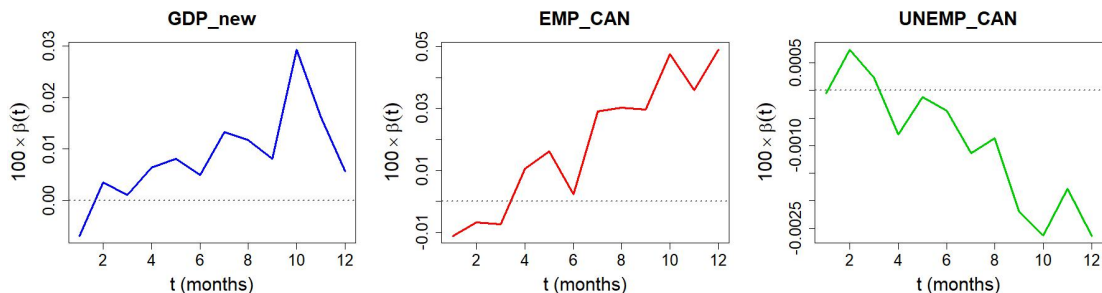


Figure 4: Estimated coefficients (β) for the three selected predictors for GDP growth.

We now compare the predictive performance of SOFIA with other time series models. To assess the forecast accuracy, we designate the final 36 months of the dataset as the test set, while the remaining observations are used for model training. We calculate the prediction error as the RMSE, given by $\sqrt{1/36 \sum_{i=1}^{36} (y_i - \hat{y}_i)^2}$, and the MAE defined by $\sum_{i=1}^{36} |y_i - \hat{y}_i|/36$, where y_i denotes the observed value in the i^{th} iteration, and \hat{y}_i is the forecast.

As benchmarks, we compare the performance of SOFIA with three alternative models: the AutoRegressive Integrated Moving Average (ARIMA), the AutoRegressive Integrated Moving Average with Exogenous Regressors (ARIMAX), and a Simple Functional (non-penalized) Regression model that uses only `GDP_new` as the functional predictor.

We estimate ARIMA and ARIMAX using the function `auto.arima()` from the R package `forecast`, which automatically selects the optimal order based on the corrected Akaike Information Criterion (AICc). We fit the models using the default settings, including the maximum values for the autoregressive and moving average orders. Then, we pass the fitted models to the `Arima()` function to generate forecasts and assess the predictive performance on the test set without reestimating the model. In ARIMAX, while the parameters for `GDP_new` are selected automatically, we include the same exogenous predictors at time $t - 1$ as in SOFIA, ensuring a fair comparison in terms of available information. Finally, we implement the Simple Functional Regression model as a minimalist functional approach, incorporating only the functional representation of `GDP_new` over the 12-month predictor window, without any penalization or variable selection.

The ARIMA model selected by `auto.arima()` is an ARIMA(4, 0, 5) with non-zero mean, while the ARIMAX model is specified as a regression with ARIMA(3,0,0) errors. Table 3 compares the RMSE and MAE values in the four models. SOFIA achieves the lowest prediction error among all the models, slightly outperforming ARIMA in both RMSE and MAE. While the ARIMAX model shows a marginal improvement in MAE compared to ARIMA, its RMSE is higher, suggesting that the inclusion of exogenous predictors does not consistently enhance forecasting accuracy. The Simple Functional Regression performs moderately well but is clearly outperformed by SOFIA, as expected. This highlights the benefit of selecting informative predictors through the SOFIA procedure rather than relying on a single functional covariate.

Table 3: RMSE and MAE comparison for different forecasting models

Model	ARIMA	ARIMAX	Simple Func. Reg	SOFIA
RMSE	0.2163	0.2361	0.2234	0.2125
MAE	0.1781	0.1742	0.1830	0.1651

7 Conclusions and future work

In this paper, we have introduced a new method, SOFIA, for variable selection in scalar-on-function regression models that estimates the coefficients with a desired level of smoothness. We search for the coefficients in an RKHS-type space that determines the smoothness level while letting the predictors live in a general Hilbert space. We have shown that SOFIA satisfies the functional oracle property, even in scenarios where the number of predictors grows exponentially compared to the sample size. In an extensive simulation study, we demonstrated the advantages of our method in variable selection and prediction accuracy.

The literature in this area is limited and there is a great space for more research. First, in our study, we assume that the functional predictors are fully observed and are not contaminated by noise. In practice, the variables are noisy and observed on a finite grid. So, considering the effect of noise and the grid size remains an open issue. Moreover, to overcome the non-invertibility of the covariance matrix in a functional context, we projected the data onto a finite-dimensional subspace, and our main results were obtained in finite-dimensional spaces. However, the optimal value of the dimension remains an open problem.

More broadly, SOFIA is a linear regression method with a lasso penalty, as time-varying data acquisition advances, the need for more complex statistical tools (nonlinear methods or more complicated penalties) will become more important. This will add many theoretical and computational

challenges, highlighting the need for ongoing research in FDA, in general, and functional regression models, specifically.

Appendix

A Proofs

This appendix contains the mathematical arguments supporting the theoretical results presented in the main text. The proofs establish several core properties of the SOFIA estimator, such as consistency, convergence toward the oracle estimator, and accurate support recovery. Each part of the appendix addresses a specific proposition or theorem and develops the proof step by step under the corresponding assumptions.

A.1 Proof of Proposition 1.

First, we show that $R(K^{1/2}) = \mathbb{K}$, and then discuss the equality of norms. Let $h \in R(K^{1/2})$. Then there exists $g \in \mathbb{H}$ such that $h = K^{1/2}(g)$. Using the self-adjointness of K and Parseval's identity, we have

$$\sum_{i=1}^{+\infty} \frac{|\langle h, v_i \rangle_{\mathbb{H}}|^2}{\theta_i} = \sum_{i=1}^{+\infty} \frac{|\langle K^{1/2}(g), v_i \rangle_{\mathbb{H}}|^2}{\theta_i} = \sum_{i=1}^{+\infty} |\langle g, v_i \rangle_{\mathbb{H}}|^2 = \|g\|_{\mathbb{H}}^2.$$

This proves that $h \in \mathbb{K}$. To prove the reverse, let $h \in \mathbb{K}$ and define $g = \sum_{i=1}^{\infty} (\langle h, v_i \rangle / \sqrt{\theta_i}) v_i$. Observe that g is well defined by the definition of \mathbb{K} . Moreover, by another use of the self-adjointness of K and Parseval's identity, we have

$$K^{1/2}(g) = K^{1/2} \left(\sum_{i=1}^{+\infty} \frac{\langle h, v_i \rangle_{\mathbb{H}} v_i}{\sqrt{\theta_i}} \right) = \sum_{i=1}^{+\infty} \langle h, v_i \rangle_{\mathbb{H}} v_i = h.$$

Therefore, $h \in R(K^{1/2})$.

The following argument shows that the two norms are equal. Let $h \in \mathbb{K} = R(K^{1/2})$. Then, there exists $g \in \mathbb{H}$ such that $K^{1/2}(g) = h$. Now, we have

$$\|h\|_{R(K^{1/2})}^2 = \|g\|_{\mathbb{H}}^2 = \sum_{i=1}^{+\infty} \langle g, v_i \rangle_{\mathbb{H}}^2 = \sum_{i=1}^{+\infty} \theta_i \frac{\langle g, v_i \rangle_{\mathbb{H}}^2}{\theta_i} = \sum_{i=1}^{+\infty} \frac{\langle h, v_i \rangle_{\mathbb{H}}^2}{\theta_i} = \|h\|_{\mathbb{K}}^2.$$

A.2 Approximation error

Proposition 2. *Let $X^{[j]}$ and β_j^* satisfy Assumption 2 for all $j \in \{1, \dots, I_0\}$. Then, as the dimension m increases, the approximation error in expression (6) tends to zero.*

Proof. The expansions of the predictors and the coefficients are

$$X_{nj} = \sum_{l=1}^{+\infty} \langle X_{nj}, v_l \rangle_{\mathbb{H}} v_l, \quad \beta_j^* = \sum_{l=1}^{+\infty} \langle \beta_j^*, v_l \rangle_{\mathbb{H}} v_l,$$

and the inner product can then be expressed as

$$\langle \beta_j^*, X_{nj} \rangle_{\mathbb{H}} = \sum_{l=1}^{+\infty} \langle \beta_j^*, v_l \rangle_{\mathbb{H}} \langle X_{nj}, v_l \rangle_{\mathbb{H}}.$$

By restricting to a finite-dimensional subspace $\mathbb{H}^{(m)}$, the latter becomes

$$\langle \beta_j^*, X_{nj} \rangle_{\mathbb{H}} = \langle \beta_j^{*(m)}, X_{nj}^{(m)} \rangle_{\mathbb{H}} + e_{nj},$$

where e_{nj} is the approximation error

$$e_{nj} = \sum_{l=m+1}^{+\infty} \langle \beta_j^*, v_l \rangle_{\mathbb{H}} \langle X_{nj}, v_l \rangle_{\mathbb{H}}.$$

Using the Cauchy-Schwarz inequality, we get

$$e_{nj}^2 = \left(\sum_{l=m+1}^{+\infty} \langle \beta_j^*, v_l \rangle_{\mathbb{H}} \langle X_{nj}, v_l \rangle_{\mathbb{H}} \right)^2 \leq \sum_{l=m+1}^{+\infty} \theta_l^{-1} \langle \beta_j^*, v_l \rangle_{\mathbb{H}}^2 \sum_{l=m+1}^{+\infty} \theta_l \langle X_{nj}, v_l \rangle_{\mathbb{H}}^2.$$

By Assumption 2, we have the bounds

$$\sum_{l=m+1}^{+\infty} \theta_l^{-1} \langle \beta_j^*, v_l \rangle_{\mathbb{H}}^2 \leq \|\beta_j^*\|_{\mathbb{K}}^2 \leq b_1^2 \quad \text{and} \quad \sum_{l=m+1}^{+\infty} \theta_l \langle X_{nj}, v_l \rangle_{\mathbb{H}}^2 \leq b_2 \sum_{l=m+1}^{+\infty} l^{-\gamma}$$

with $\gamma > 1$. By applying the integral test, there exists a constant C such that $\sum_{l=m+1}^{\infty} l^{-\gamma} \leq Cm^{-(\gamma-1)}$. As a result, the squared error is bounded as $e_{nj}^2 \leq b_1^2 b_2 C m^{-(\gamma-1)}$. Then, by the square root and summing over $j \in \mathcal{S}$, the total error satisfies

$$\sum_{j \in \mathcal{S}} e_{nj} \leq \sum_{j \in \mathcal{S}} b_1 (b_2 C)^{1/2} m^{-(\gamma-1)/2} = b_1 (b_2 C)^{1/2} I_0 m^{-(\gamma-1)/2}.$$

By the assumption $I_0 = O(m)$, there exists a constant C_I such that $I_0 \leq C_I m$. Then, we can write

$$\sum_{j \in \mathcal{S}} e_{nj} \leq \bar{C} m^{1-(\gamma-1)/2},$$

where $\bar{C} = b_1 (b_2 C)^{1/2} C_I$. Since $\gamma > 1$, this upper bound converges to zero as $m \rightarrow +\infty$. Note that, for $j \notin \mathcal{S}$, $\beta_j^* = 0$, and the approximation error vanishes. For this reason, we only consider bounds for $j \in \mathcal{S}$. □

A.3 Concentration inequality

This subsection contains the proof of Lemma 1, a kind of concentration inequality for Hilbert-valued random variables. This lemma will be used multiple times in the proofs of Theorems 1 and 2.

Proof of Lemma 1. By the Riesz representation theorem, we can represent the norm of Z as

$$\|Z\|_{\mathbb{H}} = \sup_{\|u\|_{\mathbb{H}}=1} \langle Z, u \rangle_{\mathbb{H}} = \sup_{\|u\|_{\mathbb{H}}=1} \frac{1}{N} \sum_{n=1}^N \epsilon_n \langle X_n, u \rangle_{\mathbb{H}}.$$

Fix any unit vector $u \in \mathbb{H}$, and define $a_n := \langle X_n, u \rangle_{\mathbb{H}}$ for $n = 1, \dots, N$. Then,

$$\sum_{n=1}^N a_n^2 = \sum_{n=1}^N \langle X_n, u \rangle_{\mathbb{H}}^2 \leq \sum_{n=1}^N \|X_n\|_{\mathbb{H}}^2 = N,$$

by the Cauchy–Schwarz inequality. Let $b := \sum_{n=1}^N a_n^2$, and define the normalized coefficients $\tilde{a}_n := a_n/\sqrt{b}$ so that $\sum_{n=1}^N \tilde{a}_n^2 = 1$. We can now write

$$\langle Z, u \rangle_{\mathbb{H}} = \frac{1}{N} \sum_{n=1}^N a_n \epsilon_n = \frac{\sqrt{b}}{N} \sum_{n=1}^N \tilde{a}_n \epsilon_n.$$

Then, we apply Lemma 1 from the supplementary of Huang et al. (2008) to the normalized sum $\sum_{n=1}^N \tilde{a}_n \epsilon_n$, which yields the existence of a constant M , such that for any $t > 0$,

$$P(\langle Z, u \rangle_{\mathbb{H}} > t) = P\left(\sum_{n=1}^N \tilde{a}_n \epsilon_n > \frac{Nt}{\sqrt{b}}\right) \leq \exp\left(-\frac{N^2 t^2}{bM}\right) \leq \exp\left(-\frac{Nt^2}{M}\right),$$

where the final inequality follows from $b \leq N$. Since the bound holds uniformly over all $u \in \mathbb{H}$ with $\|u\|_{\mathbb{H}} = 1$ and, by the Riesz representation theorem, there exists a unique u^* with unit norm such that $\|Z\|_{\mathbb{H}} = \langle Z, u^* \rangle_{\mathbb{H}}$, we obtain the claimed inequality.

A.4 Proof of Theorem 1

Before proving Theorem 1, we state and prove two useful lemmas. The following lemma is a direct result of Lemma 1, which establishes a uniform concentration bound over a collection of Hilbert-valued processes $\{Z_i\}_{i=1}^I$.

Lemma 2. *Let $\mathbf{X} = (X_1, \dots, X_N)$ and $\boldsymbol{\epsilon} = (\epsilon_1, \dots, \epsilon_N)$ be as in Assumption 1. For each $i = 1, \dots, I$, define $Z_i := N^{-1} \sum_{n=1}^N \epsilon_n X_{ni}$. Consider $M > 0$ from Lemma 1 and, for any $\delta \in (0, 1)$, set*

$$\lambda_0 := \sqrt{\frac{M \log(I/\delta)}{N}}.$$

Then,

$$P\left(\max_{1 \leq i \leq I} \|Z_i\|_{\mathbb{K}} \leq \lambda_0\right) \geq 1 - \delta.$$

Proof. Fix any $i \in \{1, \dots, I\}$. By Lemma 1, for all $t > 0$, we have $P(\|Z_i\|_{\mathbb{K}} > t) \leq \exp(-Nt^2/M)$. By the union bound over $i = 1, \dots, I$, we obtain

$$P\left(\max_{1 \leq i \leq I} \|Z_i\|_{\mathbb{K}} > t\right) \leq \sum_{i=1}^I P(\|Z_i\|_{\mathbb{K}} > t) \leq I \cdot \exp\left(-\frac{Nt^2}{M}\right).$$

Now set $t = \lambda_0$. Then,

$$P\left(\max_{1 \leq i \leq I} \|Z_i\|_{\mathbb{K}} > \lambda_0\right) \leq \delta.$$

□

The following lemma plays a central role in the proof of Theorem 1. It is the Hilbert-space analog of similar inequalities developed in the scalar design setting in Barber et al. (2017).

Lemma 3. Let Assumption 1 hold and $\tilde{\boldsymbol{\beta}}^{(m)}$ be a minimizer of the objective function (8) with weights equal to 1. If the tuning parameter λ satisfies

$$\lambda \geq 2 \max_{1 \leq i \leq I} \left\| \frac{1}{N} \boldsymbol{\epsilon}^\top K(\mathbf{X}^{[i]}) \right\|_{\mathbb{K}},$$

then $\tilde{\boldsymbol{\beta}}^{(m)}$ satisfies

$$\left\| \Gamma_{XX}^{(m)1/2} \left(\tilde{\boldsymbol{\beta}}^{(m)} - \boldsymbol{\beta}^{*(m)} \right) \right\|_{\mathbb{K}}^2 + \lambda \left\| \tilde{\boldsymbol{\beta}}_{\mathcal{S}^{(m)c}}^{(m)} \right\|_{\ell_1/\mathbb{K}} \leq 3\lambda \left\| \left(\tilde{\boldsymbol{\beta}}^{(m)} - \boldsymbol{\beta}^{*(m)} \right)_{\mathcal{S}^{(m)}} \right\|_{\ell_1/\mathbb{K}}.$$

Proof. For $i, j = 1, \dots, I$, we use the notation $K(\mathbf{X}^{(m)})_{ij} = K(X_{ij}^{(m)})$. The expression $\langle K(\mathbf{X}^{(m)}), \boldsymbol{\beta} \rangle_{\mathbb{K}}$ represents a vector in \mathbb{R}^N , whose n^{th} element is equal to $\sum_{i=1}^I \langle K(\mathbf{X}_{ni}^{(m)}), \beta_i \rangle_{\mathbb{K}}$. Since $\tilde{\boldsymbol{\beta}}^{(m)}$ is the minimizer, we have

$$\frac{1}{2N} \left| Y - \left\langle K(\mathbf{X}^{(m)}), \tilde{\boldsymbol{\beta}}^{(m)} \right\rangle_{\mathbb{K}} \right|^2 + \lambda \left\| \tilde{\boldsymbol{\beta}}^{(m)} \right\|_{\ell_1/\mathbb{K}} \leq \frac{1}{2N} \left| Y - \left\langle K(\mathbf{X}^{(m)}), \boldsymbol{\beta}^{*(m)} \right\rangle_{\mathbb{K}} \right|^2 + \lambda \left\| \boldsymbol{\beta}^{*(m)} \right\|_{\ell_1/\mathbb{K}},$$

where $|\cdot|$ is the Euclidean norm in \mathbb{R}^N . Additionally,

$$\begin{aligned} \frac{1}{2} \left| Y - \left\langle K(\mathbf{X}^{(m)}), \tilde{\boldsymbol{\beta}}^{(m)} \right\rangle_{\mathbb{K}} \right|^2 &= \frac{1}{2} \left| Y - \left\langle K(\mathbf{X}^{(m)}), \boldsymbol{\beta}^{*(m)} \right\rangle_{\mathbb{K}} \right|^2 + \frac{1}{2} \left| \left\langle K(\mathbf{X}^{(m)}), \tilde{\boldsymbol{\beta}}^{(m)} - \boldsymbol{\beta}^{*(m)} \right\rangle_{\mathbb{K}} \right|^2 \\ &\quad - \left(Y - \left\langle K(\mathbf{X}^{(m)}), \boldsymbol{\beta}^{*(m)} \right\rangle_{\mathbb{K}} \right) \left(\left\langle K(\mathbf{X}^{(m)}), \tilde{\boldsymbol{\beta}}^{(m)} - \boldsymbol{\beta}^{*(m)} \right\rangle_{\mathbb{K}} \right)^\top. \end{aligned}$$

By the definition of norm, expanding the inner product and rearranging terms, we get

$$\begin{aligned} &\frac{1}{2} \left\| \Gamma_{XX}^{(m)1/2} \left(\tilde{\boldsymbol{\beta}}^{(m)} - \boldsymbol{\beta}^{*(m)} \right) \right\|_{\mathbb{K}}^2 + \lambda \left\| \tilde{\boldsymbol{\beta}}^{(m)} \right\|_{\ell_1/\mathbb{K}} \\ &\leq \sum_{i=1}^I \left\langle \frac{1}{N} \boldsymbol{\epsilon}^\top K(\mathbf{X}^{(m)[i]}), \tilde{\beta}_i^{(m)} - \beta_i^{*(m)} \right\rangle_{\mathbb{K}} + \lambda \left\| \boldsymbol{\beta}^{*(m)} \right\|_{\ell_1/\mathbb{K}} \\ &\leq \sum_{i=1}^I \left\| \frac{1}{N} \boldsymbol{\epsilon}^\top K(\mathbf{X}^{[i]}) \right\|_{\mathbb{K}} \left\| \tilde{\beta}_i^{(m)} - \beta_i^{*(m)} \right\|_{\mathbb{K}} + \lambda \left\| \boldsymbol{\beta}^{*(m)} \right\|_{\ell_1/\mathbb{K}} \\ &\leq \left(\max_{1 \leq i \leq I} \left\| \frac{1}{N} \boldsymbol{\epsilon}^\top K(\mathbf{X}^{[i]}) \right\|_{\mathbb{K}} \right) \left\| \tilde{\boldsymbol{\beta}}^{(m)} - \boldsymbol{\beta}^{*(m)} \right\|_{\ell_1/\mathbb{K}} + \lambda \left\| \boldsymbol{\beta}^{*(m)} \right\|_{\ell_1/\mathbb{K}}. \end{aligned}$$

By using this inequality, we conclude that,

$$\left\| \Gamma_{XX}^{(m)1/2} \left(\tilde{\boldsymbol{\beta}}^{(m)} - \boldsymbol{\beta}^{*(m)} \right) \right\|_{\mathbb{K}}^2 + 2\lambda \left\| \tilde{\boldsymbol{\beta}}^{(m)} \right\|_{\ell_1/\mathbb{K}} \leq \lambda \left\| \tilde{\boldsymbol{\beta}}^{(m)} - \boldsymbol{\beta}^{*(m)} \right\|_{\ell_1/\mathbb{K}} + 2\lambda \left\| \boldsymbol{\beta}^{*(m)} \right\|_{\ell_1/\mathbb{K}}. \quad (12)$$

Obviously, $\left\| \tilde{\boldsymbol{\beta}}^{(m)} \right\|_{\ell_1/\mathbb{K}} = \left\| \tilde{\boldsymbol{\beta}}_{\mathcal{S}^{(m)}}^{(m)} \right\|_{\ell_1/\mathbb{K}} + \left\| \tilde{\boldsymbol{\beta}}_{\mathcal{S}^{(m)c}}^{(m)} \right\|_{\ell_1/\mathbb{K}}$. Moreover, by the reverse triangle inequality,

$$\left\| \tilde{\boldsymbol{\beta}}_{\mathcal{S}^{(m)}}^{(m)} \right\|_{\ell_1/\mathbb{K}} \geq \left\| \boldsymbol{\beta}_{\mathcal{S}^{(m)}}^{*(m)} \right\|_{\ell_1/\mathbb{K}} - \left\| \tilde{\boldsymbol{\beta}}_{\mathcal{S}^{(m)}}^{(m)} - \boldsymbol{\beta}_{\mathcal{S}^{(m)}}^{*(m)} \right\|_{\ell_1/\mathbb{K}}.$$

Combining these, we get

$$\left\| \tilde{\boldsymbol{\beta}}^{(m)} \right\|_{\ell_1/\mathbb{K}} \geq \left\| \boldsymbol{\beta}_{\mathcal{S}^{(m)}}^{*(m)} \right\|_{\ell_1/\mathbb{K}} - \left\| \tilde{\boldsymbol{\beta}}_{\mathcal{S}^{(m)}}^{(m)} - \boldsymbol{\beta}_{\mathcal{S}^{(m)}}^{*(m)} \right\|_{\ell_1/\mathbb{K}} + \left\| \tilde{\boldsymbol{\beta}}_{\mathcal{S}^{(m)c}}^{(m)} \right\|_{\ell_1/\mathbb{K}}.$$

Also, note that

$$\left\| \tilde{\beta}^{(m)} - \beta^{*(m)} \right\|_{\ell_1/\mathbb{K}} = \left\| \tilde{\beta}^{(m)} - \beta_{\mathcal{S}^{(m)}}^{*(m)} \right\|_{\ell_1/\mathbb{K}} + \left\| \tilde{\beta}_{\mathcal{S}^{(m)C}}^{(m)} \right\|_{\ell_1/\mathbb{K}}.$$

By substitution into inequality (12), we conclude

$$\begin{aligned} \left\| \Gamma_{XX}^{(m)1/2} \left(\tilde{\beta}^{(m)} - \beta^{*(m)} \right) \right\|_{\mathbb{K}}^2 &\leq \lambda \left\| \tilde{\beta}^{(m)} - \beta^{*(m)} \right\|_{\ell_1/\mathbb{K}} + 2\lambda \left\| \beta^{*(m)} \right\|_{\ell_1/\mathbb{K}} - 2\lambda \left\| \tilde{\beta}^{(m)} \right\|_{\ell_1/\mathbb{K}} \\ &\leq \lambda \left(\left\| \tilde{\beta}_{\mathcal{S}^{(m)}}^{(m)} - \beta_{\mathcal{S}^{(m)}}^{*(m)} \right\|_{\ell_1/\mathbb{K}} + \left\| \tilde{\beta}_{\mathcal{S}^{(m)C}}^{(m)} \right\|_{\ell_1/\mathbb{K}} \right) + 2\lambda \left\| \beta_{\mathcal{S}^{(m)C}}^{*(m)} \right\|_{\ell_1/\mathbb{K}} \\ &\quad - 2\lambda \left(\left\| \beta_{\mathcal{S}^{(m)}}^{*(m)} \right\|_{\ell_1/\mathbb{K}} - \left\| \tilde{\beta}_{\mathcal{S}^{(m)}}^{(m)} - \beta_{\mathcal{S}^{(m)}}^{*(m)} \right\|_{\ell_1/\mathbb{K}} + \left\| \tilde{\beta}_{\mathcal{S}^{(m)C}}^{(m)} \right\|_{\ell_1/\mathbb{K}} \right). \end{aligned}$$

Simplification and rearrangement yield the desired result. \square

Proof of Theorem 1. We start with the decomposition

$$\begin{aligned} \left\| \Gamma_{XX}^{(m)1/2} \left(\tilde{\beta}^{(m)} - \beta^{*(m)} \right) \right\|_{\mathbb{K}}^2 + \lambda \left\| \tilde{\beta}^{(m)} - \beta^{*(m)} \right\|_{\ell_1/\mathbb{K}} &= \left\| \Gamma_{XX}^{(m)1/2} \left(\tilde{\beta}^{(m)} - \beta^{*(m)} \right) \right\|_{\mathbb{K}}^2 \\ &\quad + \lambda \left\| \left(\tilde{\beta}^{(m)} - \beta^{*(m)} \right)_{\mathcal{S}^{(m)}} \right\|_{\ell_1/\mathbb{K}} + \lambda \left\| \tilde{\beta}_{\mathcal{S}^{(m)C}}^{(m)} \right\|_{\ell_1/\mathbb{K}}. \end{aligned}$$

By using Lemmas 2 and 3, with probability at least $1 - \delta$, we have

$$\begin{aligned} \left\| \Gamma_{XX}^{(m)1/2} \left(\tilde{\beta}^{(m)} - \beta^{*(m)} \right) \right\|_{\mathbb{K}}^2 + \lambda \left\| \left(\tilde{\beta}^{(m)} - \beta^{*(m)} \right)_{\mathcal{S}^{(m)}} \right\|_{\ell_1/\mathbb{K}} + \lambda \left\| \tilde{\beta}_{\mathcal{S}^{(m)C}}^{(m)} \right\|_{\ell_1/\mathbb{K}} &\quad (13) \\ &\leq 4\lambda \left\| \left(\tilde{\beta}^{(m)} - \beta^{*(m)} \right)_{\mathcal{S}^{(m)}} \right\|_{\ell_1/\mathbb{K}}. \end{aligned}$$

Now, using the relationship between the ℓ_1 and ℓ_2 norms, we can further bound the right-hand side:

$$4\lambda \left\| \left(\tilde{\beta}^{(m)} - \beta^{*(m)} \right)_{\mathcal{S}^{(m)}} \right\|_{\ell_1/\mathbb{K}} \leq 4\lambda\sqrt{I_0} \left\| \left(\tilde{\beta}^{(m)} - \beta^{*(m)} \right)_{\mathcal{S}^{(m)}} \right\|_{\mathbb{K}}.$$

Next, we use Assumption 3:

$$4\lambda\sqrt{I_0} \left\| \left(\tilde{\beta}^{(m)} - \beta^{*(m)} \right)_{\mathcal{S}^{(m)}} \right\|_{\mathbb{K}} \leq \frac{4\lambda\sqrt{I_0}}{\alpha_m} \left\| \Gamma_{XX}^{(m)1/2} \left(\tilde{\beta}^{(m)} - \beta^{*(m)} \right) \right\|_{\mathbb{K}}.$$

Using the inequality $2ab \leq a^2 + b^2$ for real numbers, we further bound the right-hand side:

$$\frac{4\lambda\sqrt{I_0}}{\alpha_m} \left\| \Gamma_{XX}^{(m)1/2} \left(\tilde{\beta}^{(m)} - \beta^{*(m)} \right) \right\|_{\mathbb{K}} \leq \frac{1}{2} \left\| \Gamma_{XX}^{(m)1/2} \left(\tilde{\beta}^{(m)} - \beta^{*(m)} \right) \right\|_{\mathbb{K}}^2 + \frac{8\lambda^2 I_0}{\alpha_m^2}.$$

By substitution in the inequality (13), we obtain

$$\begin{aligned} \left\| \Gamma_{XX}^{(m)1/2} \left(\tilde{\beta}^{(m)} - \beta^{*(m)} \right) \right\|_{\mathbb{K}}^2 + \lambda \left\| \left(\tilde{\beta}^{(m)} - \beta^{*(m)} \right)_{\mathcal{S}^{(m)}} \right\|_{\ell_1/\mathbb{K}} + \lambda \left\| \tilde{\beta}_{\mathcal{S}^{(m)C}}^{(m)} \right\|_{\ell_1/\mathbb{K}} & \\ &\leq \frac{1}{2} \left\| \Gamma_{XX}^{(m)1/2} \left(\tilde{\beta}^{(m)} - \beta^{*(m)} \right) \right\|_{\mathbb{K}}^2 + \frac{8\lambda^2 I_0}{\alpha_m^2}. \end{aligned}$$

Rearranging terms, we conclude that, with probability at least $1 - \delta$,

$$\frac{1}{2} \left\| \Gamma_{XX}^{(m)1/2} \left(\tilde{\beta}^{(m)} - \beta^{*(m)} \right) \right\|_{\mathbb{K}}^2 + \lambda \left\| \tilde{\beta}^{(m)} - \beta^{*(m)} \right\|_{\ell_1/\mathbb{K}} \leq \frac{8\lambda^2 I_0}{\alpha_m^2}.$$

This completes the proof.

A.5 Functional subgradient

To prove Theorem 2, we first compute the functional subgradient of the objective function (8). The following lemma establishes a simple yet crucial connection between the inner products on \mathbb{H} and \mathbb{K} , allowing us to bridge the gap between these spaces.

Lemma 4. *Let $x \in \mathbb{K}$ and $z \in \mathbb{H}$. Then, the subgradient of $\langle x, z \rangle_{\mathbb{H}}$ with respect to x on \mathbb{K} is the singleton $\{K(z)\}$.*

Proof. From Proposition 1, we know that, for $z \in \mathbb{H}$, the relation $\|K^{1/2}(z)\|_{\mathbb{K}} = \|z\|_{\mathbb{H}}$ holds. Using the polarization identity, we express the inner product in terms of the norm:

$$\begin{aligned} \langle x, z \rangle_{\mathbb{H}} &= \frac{1}{4} \left(\|x + z\|_{\mathbb{H}}^2 - \|x - z\|_{\mathbb{H}}^2 \right) = \frac{1}{4} \left(\|K^{1/2}(x + z)\|_{\mathbb{K}}^2 - \|K^{1/2}(x - z)\|_{\mathbb{K}}^2 \right) \\ &= \left\langle K^{1/2}(x), K^{1/2}(z) \right\rangle_{\mathbb{K}} = \langle x, K(z) \rangle_{\mathbb{K}}. \end{aligned}$$

Now, let $f(x) = \langle x, z \rangle_{\mathbb{H}}$. For any $y \in \mathbb{K}$

$$f(x + y) - f(x) = \langle x + y, z \rangle_{\mathbb{H}} - \langle x, z \rangle_{\mathbb{H}} = \langle y, z \rangle_{\mathbb{H}} = \langle K(z), y \rangle_{\mathbb{K}}.$$

Thus, $K(z)$ is a subgradient of f at x . To show that $K(z)$ is the full subdifferential of f at x , consider $w \neq K(z)$ in \mathbb{K} . By the Riesz representation theorem, there exists a $y \in \mathbb{K}$ such that $\langle y, K(z) - w \rangle_{\mathbb{K}} \neq 0$. This implies that no other vector $w \neq K(z)$ satisfies the subgradient inequality for all y . \square

Now, we can compute the subgradient of function (8) using basic tools from convex analysis. For the square error part of the objective function, the subgradient can be computed using the Lemma 4, combined with the additivity and linearity of subdifferentials, in the following way:

$$\frac{\partial}{\partial \beta_i} \frac{1}{2N} \sum_{n=1}^N \left(Y_n - \sum_{j=1}^I \langle \beta_j, X_{nj}^{(m)} \rangle_{\mathbb{H}} \right)^2 = -\frac{1}{N} \left(\sum_{n=1}^N \left(Y_n - \sum_{j=1}^I \langle \beta_j, K(X_{nj}^{(m)}) \rangle_{\mathbb{K}} \right) K(X_{ni}^{(m)}) \right).$$

The subgradient of the second part can be computed using Section A.1 in Fan and Reimherr (2017):

$$\frac{\partial}{\partial \beta_i} \lambda \sum_{j=1}^I \tilde{w}_j \|\beta_j\|_{\mathbb{K}} = \lambda \tilde{w}_i \begin{cases} \|\beta_i\|_{\mathbb{K}}^{-1} \beta_i & \text{if } \beta_i \neq 0, \\ \{h \in \mathbb{H} : \|h\|_{\mathbb{K}} \leq 1\} & \text{if } \beta_i = 0. \end{cases}$$

Finally, the subgradient of the entire function is the sum of these two:

$$\begin{aligned} \frac{\partial}{\partial \beta_i} L_{\lambda}(\boldsymbol{\beta}) &= -\frac{1}{N} \left(\sum_{n=1}^N \left(Y_n - \sum_{j=1}^I \langle \beta_j, K(X_{nj}^{(m)}) \rangle_{\mathbb{K}} \right) K(X_{ni}^{(m)}) \right) \\ &\quad + \lambda \tilde{w}_i \begin{cases} \|\beta_i\|_{\mathbb{K}}^{-1} \beta_i & \text{if } \beta_i \neq 0, \\ \{h \in \mathbb{K} : \|h\|_{\mathbb{K}} \leq 1\} & \text{if } \beta_i = 0. \end{cases} \end{aligned}$$

Note that β_i is an element of $\mathbb{K}^{(m)}$ and the function L_{λ} is defined over $\mathbb{K}^{(m)}$. Therefore, the subgradient is a set of elements of $\mathbb{K}^{(m)}$.

A.6 Proof of Theorem 2

(i). We aim to show that, as the sample size grows, with probability tending to 1, the following holds:

$$\hat{\beta}_i^{(m)} \neq 0 \quad \text{for } i \in \mathcal{S}^{(m)} \quad \text{and} \quad \hat{\beta}_i^{(m)} = 0 \quad \text{for } i \in \mathcal{S}^{(m)c}.$$

where $\mathcal{S}^{(m)c}$ is the complement of $\mathcal{S}^{(m)}$ in $\{1, \dots, I\}$.

Consider the event $\{\hat{\mathcal{S}}^{(m)} = \mathcal{S}^{(m)}\}$. From Appendix A.5 we see that, for all $i = 1, \dots, I$,

$$\sum_{n=1}^N \left(\left(Y_n - \sum_{j \in \mathcal{S}^{(m)}} \langle \hat{\beta}_j^{(m)}, K(X_{nj}^{(m)}) \rangle_{\mathbb{K}} \right) K(X_{ni}^{(m)}) \right) = \lambda \tilde{s}_i,$$

where

$$\tilde{s}_i = N\lambda \tilde{w}_i \begin{cases} \left\| \hat{\beta}_j^{(m)} \right\|_{\mathbb{K}}^{-1} \hat{\beta}_j^{(m)} & \text{if } \hat{\beta}_j^{(m)} \neq 0 \\ \{h \in H : \|h\|_{\mathbb{K}} \leq 1\} & \text{if } \hat{\beta}_j^{(m)} = 0. \end{cases}$$

Using the relation (7), we can write

$$Y_n - \sum_{j \in \mathcal{S}^{(m)}} \langle \hat{\beta}_j^{(m)}, K(X_{nj}^{(m)}) \rangle_{\mathbb{K}} = \epsilon_n - \sum_{j \in \mathcal{S}^{(m)}} \langle \hat{\beta}_j^{(m)} - \beta_j^{*(m)}, K(X_{nj}^{(m)}) \rangle_{\mathbb{K}}.$$

By substitution, we get

$$\sum_{n=1}^N \left(\epsilon_n - \sum_{j \in \mathcal{S}^{(m)}} \langle \hat{\beta}_j^{(m)} - \beta_j^{*(m)}, K(X_{nj}^{(m)}) \rangle_{\mathbb{K}} \right) K(X_{ni}^{(m)}) = \lambda \tilde{s}_i.$$

Let $Z_i = \sum_{n=1}^N \epsilon_n X_{ni}^{(m)}$. Then,

$$K(Z_i) - \sum_{n=1}^N \sum_{j \in \mathcal{S}^{(m)}} \left(\langle \hat{\beta}_j^{(m)} - \beta_j^{*(m)}, K(X_{nj}^{(m)}) \rangle_{\mathbb{K}} K(X_{ni}^{(m)}) \right) = \lambda \tilde{s}_i.$$

Now, the tensor product definition of the covariance operator gives

$$K(Z_i) - \sum_{j \in \mathcal{S}^{(m)}} N \Gamma_{ij}^{(m)} \left(\hat{\beta}_j^{(m)} - \beta_j^{*(m)} \right) = \lambda \tilde{s}_i. \quad (14)$$

This equation restricted to $i \in \mathcal{S}^{(m)}$, with a matrix form, becomes

$$N \Gamma_{X_1}^{(m)} \left(\hat{\beta}_1^{(m)} - \beta_1^{*(m)} \right) = K(\mathbf{Z}_1) - \lambda \tilde{s}_1,$$

where $\mathbf{Z}_1 = \{Z_i : i \in \mathcal{S}^{(m)}\}$, $\hat{\beta}_1^{(m)} = \{\hat{\beta}_i^{(m)} : i \in \mathcal{S}^{(m)}\}$ and

$$\tilde{s}_1 = \left\{ N \tilde{w}_i \hat{\beta}_i^{(m)} \left\| \hat{\beta}_i^{(m)} \right\|_{\mathbb{K}}^{-1} : i \in \mathcal{S}^{(m)} \right\}.$$

So, the difference between the estimated and the true active coefficients can be formulated as

$$\hat{\beta}_1^{(m)} - \beta_1^{*(m)} = N^{-1} \Gamma_{X_1}^{(m)-1} (K(\mathbf{Z}_1) - \lambda \tilde{s}_1). \quad (15)$$

However, trivially, $\hat{\beta}_i^{(m)} \neq 0$ if

$$\left\| \beta_i^{*(m)} - \hat{\beta}_i^{(m)} \right\|_{\mathbb{K}} < \left\| \beta_i^{*(m)} \right\|_{\mathbb{K}}.$$

By substituting eq. (15) in the latter, we have to show that

$$\left\| e_i^\top N^{-1} \Gamma_{X_1}^{(m)-1} K(\mathbf{Z}_1) - e_i^\top N^{-1} \Gamma_{X_1}^{(m)-1} (\lambda \tilde{s}_1) \right\|_{\mathbb{K}} < \left\| \beta_i^{*(m)} \right\|_{\mathbb{K}}, \quad (16)$$

where e_i is a vector with 1 in the i^{th} coordinate and zero everywhere else.

Now, we move to the null part. For $i \in \mathcal{S}^{(m)c}$, we have to show that $\hat{\beta}_i^{(m)}$ is equal to zero. From eq. (14), it is sufficient to prove that

$$\left\| K(Z_i) - N \sum_{j \in \mathcal{S}^{(m)}} \Gamma_{ij}^{(m)} \left(\hat{\beta}_j^{(m)} - \beta_j^{*(m)} \right) \right\|_{\mathbb{K}} < N \lambda \tilde{w}_i.$$

In matrix notation, we can write

$$\left\| K(Z_i) - N e_i^\top \Gamma_{X_2 X_1}^{(m)} \left(\hat{\beta}_1^{(m)} - \beta_1^{*(m)} \right) \right\|_{\mathbb{K}} < N \lambda \tilde{w}_i.$$

This can be written in the form

$$\left\| K(Z_i) - e_i^\top \Gamma_{X_2 X_1}^{(m)} \Gamma_{X_1}^{(m)-1} (K(\mathbf{Z}_1) - \tilde{s}_1) \right\|_{\mathbb{K}} < N \lambda \tilde{w}_i,$$

or

$$\left\| \left(K(Z_i) - e_i^\top \Gamma_{X_2 X_1}^{(m)} \Gamma_{X_1}^{(m)-1} K(\mathbf{Z}_1) \right) + e_i^\top \Gamma_{X_2 X_1}^{(m)} \Gamma_{X_1}^{(m)-1} (\tilde{s}_1) \right\|_{\mathbb{K}} < N \lambda \tilde{w}_i. \quad (17)$$

The relations (16) and (17) indicate that $\hat{\mathcal{S}}^{(m)} = \mathcal{S}^{(m)}$ if the following two inequalities are satisfied:

$$\begin{cases} N^{-1} \left\| e_i^\top \Gamma_{X_1}^{(m)-1} K(\mathbf{Z}_1) - e_i^\top \Gamma_{X_1}^{(m)-1} (\lambda \tilde{s}_1) \right\|_{\mathbb{K}} < \left\| \beta_i^{*(m)} \right\|_{\mathbb{K}}, & i \in \mathcal{S}^{(m)}, \\ \left\| \left(K(Z_i) - e_i^\top \Gamma_{X_2 X_1}^{(m)} \Gamma_{X_1}^{(m)-1} K(\mathbf{Z}_1) \right) + e_i^\top \Gamma_{X_2 X_1}^{(m)} \Gamma_{X_1}^{(m)-1} (\tilde{s}_1) \right\|_{\mathbb{K}} < N \lambda \tilde{w}_i, & i \in \mathcal{S}^{(m)c}. \end{cases}$$

Considering the event $\{\hat{\mathcal{S}}^{(m)} \neq \mathcal{S}^{(m)}\}$, we observe that

$$\left\{ \hat{\mathcal{S}}^{(m)} \neq \mathcal{S}^{(m)} \right\} \subset B_1 \cup B_2 \cup B_3 \cup B_4,$$

where B_1, \dots, B_4 are the following subsets of indices:

$$\begin{aligned} B_1 &= \left\{ i \in \mathcal{S}^{(m)} : N^{-1} \left\| e_i^\top \hat{\Gamma}_{X_1}^{(m)-1} K(\mathbf{Z}_1) \right\|_{\mathbb{K}} \geq \frac{\left\| \beta_i^{*(m)} \right\|_{\mathbb{K}}}{2} \right\}, \\ B_2 &= \left\{ i \in \mathcal{S}^{(m)} : N^{-1} \lambda \left\| e_i^\top \hat{\Gamma}_{X_1}^{(m)-1} \tilde{s}_1 \right\|_{\mathbb{K}} \geq \frac{\left\| \beta_i^{*(m)} \right\|_{\mathbb{K}}}{2} \right\}, \\ B_3 &= \left\{ i \in \mathcal{S}^{(m)c} : N^{-1} \left\| K(Z_i) - e_i^\top \Gamma_{X_2 X_1}^{(m)} \Gamma_{X_1}^{(m)-1} K(\mathbf{Z}_1) \right\|_{\mathbb{K}} \geq \frac{\lambda \tilde{w}_i}{2} \right\}, \\ B_4 &= \left\{ i \in \mathcal{S}^{(m)c} : N^{-1} \left\| e_i^\top \Gamma_{X_2 X_1}^{(m)} \Gamma_{X_1}^{(m)-1} \tilde{s}_1 \right\|_{\mathbb{K}} \geq \frac{\tilde{w}_i}{2} \right\}. \end{aligned}$$

We show that $\lim_{N \rightarrow +\infty} P(B_l) \rightarrow 0$ for $l = 1, \dots, 4$ in separate steps. This will complete the proof of (i).

Step 1: $P(B_1) \rightarrow 0$, when $N \rightarrow +\infty$.

First, observe that, from point 1 in Assumption 4,

$$\left\| e_i^\top \hat{\Gamma}_{X_1}^{(m)-1} K(\mathbf{Z}_1) \right\|_{\mathbb{K}} \leq \theta_1 \tau_m \|\mathbf{Z}_1\|_{\mathbb{H}} \leq \theta_1 \tau_m \sum_{i \in \mathcal{S}^{(m)}} \|Z_i\|_{\mathbb{H}} \quad \forall i \in \mathcal{S}^{(m)}.$$

By point 2 of Assumption 4 (minimum signal condition),

$$P(B_1) \leq \sum_{i \in \mathcal{S}^{(m)}} P \left(N^{-1} \theta_1 \tau_m \|Z_i\|_{\mathbb{H}} \geq \frac{b_m}{2} \right).$$

Next, using the definition of Z_i , Assumption 1 and Lemma 1, we obtain

$$\begin{aligned} P(B_1) &\leq \sum_{i \in \mathcal{S}^{(m)}} P \left(N^{-1} \left\| \sum_{n=1}^N \epsilon_n X_{ni}^{(m)} \right\|_{\mathbb{H}} \geq \frac{b_m}{2\theta_1 \tau_m} \right) \leq \sum_{i \in \mathcal{S}^{(m)}} \exp \left(-\frac{b_m^2 N}{4\theta_1^2 \tau_m^2 M} \right) \\ &\leq I_0 \exp \left(-\frac{b_m^2 N}{4\theta_1^2 \tau_m^2 M} \right) = \exp \left(-\frac{b_m^2 N}{4\theta_1^2 \tau_m^2 M} + \log(I_0) \right). \end{aligned}$$

The last term tends to zero, as $N \rightarrow +\infty$, because, by the minimum signal assumption, $\log(I_0) \ll b_m^2 N / \tau_m^2$.

Step 2: $P(B_2) \rightarrow 0$, when $N \rightarrow +\infty$.

We begin by evaluating the \mathbb{K} -norm of \tilde{s}_1 :

$$\|\tilde{s}_1\|_{\mathbb{K}}^2 = N^2 \sum_{i \in \mathcal{S}^{(m)}} \tilde{w}_i^2 = N^2 \sum_{i \in \mathcal{S}^{(m)}} w_i^2 + N^2 \sum_{i \in \mathcal{S}^{(m)}} (\tilde{w}_i^2 - w_i^2),$$

where $\tilde{w}_i = \|\tilde{\beta}_i^{(m)}\|_{\mathbb{K}}^{-1}$ and $w_i = \|\beta_i^{*(m)}\|_{\mathbb{K}}^{-1}$. For the difference $\tilde{w}_i^2 - w_i^2$, we write

$$\tilde{w}_i^2 - w_i^2 = \|\tilde{\beta}_i^{(m)}\|_{\mathbb{K}}^{-2} - \|\beta_i^{*(m)}\|_{\mathbb{K}}^{-2} = \frac{\|\beta_i^{*(m)}\|_{\mathbb{K}}^2 - \|\tilde{\beta}_i^{(m)}\|_{\mathbb{K}}^2}{\|\beta_i^{*(m)}\|_{\mathbb{K}}^2 \|\tilde{\beta}_i^{(m)}\|_{\mathbb{K}}^2}.$$

By factoring in the numerator, we have

$$\tilde{w}_i^2 - w_i^2 = \frac{\left(\|\beta_i^{*(m)}\|_{\mathbb{K}} - \|\tilde{\beta}_i^{(m)}\|_{\mathbb{K}} \right) \left(\|\beta_i^{*(m)}\|_{\mathbb{K}} + \|\tilde{\beta}_i^{(m)}\|_{\mathbb{K}} \right)}{\|\beta_i^{*(m)}\|_{\mathbb{K}}^2 \|\tilde{\beta}_i^{(m)}\|_{\mathbb{K}}^2}. \quad (18)$$

From Assumption 4 and Corollary 1, we know that $r_N^{1/2}/b_m \rightarrow 0$ when $N \rightarrow +\infty$. So,

$$\|\tilde{\beta}_i^{(m)}\|_{\mathbb{K}} \leq \|\beta_i^{*(m)}\|_{\mathbb{K}} + \|\tilde{\beta}_i^{(m)} - \beta_i^{*(m)}\|_{\mathbb{K}} = \|\beta_i^{*(m)}\|_{\mathbb{K}} (1 + o_P(1))$$

uniformly in i . By the reverse triangle inequality, we similarly find

$$\|\tilde{\beta}_i^{(m)}\|_{\mathbb{K}} \geq \|\beta_i^{*(m)}\|_{\mathbb{K}} - \|\tilde{\beta}_i^{(m)} - \beta_i^{*(m)}\|_{\mathbb{K}} = \|\beta_i^{*(m)}\|_{\mathbb{K}} (1 + o_P(1)).$$

Therefore,

$$\left| \left\| \beta_i^{*(m)} \right\|_{\mathbb{K}} - \left\| \tilde{\beta}_i^{(m)} \right\|_{\mathbb{K}} \right| \leq \left\| \tilde{\beta}_i^{(m)} - \beta_i^{*(m)} \right\|_{\mathbb{K}}.$$

By substituting these relations into eq. (18), we obtain

$$|\tilde{w}_i^2 - w_i^2| = \frac{\left\| \beta_i^{*(m)} - \tilde{\beta}_i^{(m)} \right\|_{\mathbb{K}}}{\left\| \beta_i^{*(m)} \right\|_{\mathbb{K}}^3} (2 + o_P(1))$$

uniformly in i . Using the bound $b_m \leq \|\beta_i^{*(m)}\|_{\mathbb{K}}$ for all $i \in \mathcal{S}^{(m)}$, we find

$$|\tilde{w}_i^2 - w_i^2| \leq \frac{O_P(1)}{\left\| \beta_i^{*(m)} \right\|_{\mathbb{K}}^2 b_m} \left\| \beta_i^{*(m)} - \tilde{\beta}_i^{(m)} \right\|_{\mathbb{K}} \leq \frac{O_P\left(r_N^{1/2}\right)}{b_m} w_i^2.$$

Since $r_N^{1/2}/b_m \rightarrow 0$ when $N \rightarrow +\infty$, we conclude

$$\begin{aligned} \|\tilde{s}_1\|_{\mathbb{K}}^2 &\leq N^2 \left(\sum_{i \in \mathcal{S}^{(m)}} w_i^2 \right) (1 + o_P(1)) = N^2 \left(\sum_{i \in \mathcal{S}^{(m)}} \frac{1}{\left\| \beta_i^{*(m)} \right\|_{\mathbb{K}}^2} \right) (1 + o_P(1)) \\ &\leq \frac{N^2 I_0}{b_m^2} (1 + o_P(1)). \end{aligned} \tag{19}$$

Now we return to the definition of B_2 . For each $i \in \mathcal{S}^{(m)}$,

$$\left\| e_i^\top \hat{\Gamma}_{X_1}^{(m)-1} \tilde{s}_1 \right\|_{\mathbb{K}} \leq \tau_m \|\tilde{s}_1\|_{\mathbb{K}} \leq \frac{\tau_m N I_0^{1/2}}{b_m} (1 + o_P(1)).$$

Hence,

$$\begin{aligned} P(B_2) &\leq \sum_{i \in \mathcal{S}^{(m)}} P \left(N^{-1} \lambda \left\| e_i^\top \hat{\Gamma}_{X_1}^{(m)-1} \tilde{s}_1 \right\|_{\mathbb{K}} \geq \frac{\left\| \beta_i^{*(m)} \right\|_{\mathbb{K}}}{2} \right) \\ &\leq \sum_{i \in \mathcal{S}^{(m)}} P \left(\lambda \frac{\tau_m N I_0^{1/2}}{b_m N} (1 + o_P(1)) \geq \frac{b_m}{2} \right). \end{aligned}$$

By simplifying further, using point 4 in Assumption 4 and the fact that $I_0 \ll N$, we have

$$P(B_2) \leq I_0 P \left(\lambda \geq \frac{b_m^2}{\tau_m I_0^{1/2}} \right) \rightarrow 0, \quad N \rightarrow +\infty.$$

Step 3: $P(B_3) \rightarrow 0$, when $N \rightarrow +\infty$.

For each $i \in \mathcal{S}^{(m)c}$, we define the event

$$A_i = \left\{ N^{-1} \left\| K(Z_i) - e_i^\top \Gamma_{X_2 X_1}^{(m)} \Gamma_{X_1}^{(m)-1} K(\mathbf{Z}_1) \right\|_{\mathbb{K}} \geq \frac{\lambda \tilde{w}_i}{2} \right\}.$$

We observe that

$$\left\| K(Z_i) - e_i^\top \Gamma_{X_2 X_1}^{(m)} \Gamma_{X_1}^{(m)-1} K(\mathbf{Z}_1) \right\|_{\mathbb{K}} \leq \|K(Z_i)\|_{\mathbb{K}} + \left\| e_i^\top \Gamma_{X_2 X_1}^{(m)} \Gamma_{X_1}^{(m)-1} K(\mathbf{Z}_1) \right\|_{\mathbb{K}}.$$

Using this bound, we can write $A_i \subseteq A_{i,1} \cup A_{i,2}$, where

$$A_{i,1} = \left\{ N^{-1} \|K(Z_i)\|_{\mathbb{K}} \geq \frac{\lambda \tilde{w}_i}{4} \right\},$$

$$A_{i,2} = \left\{ N^{-1} \left\| e_i^\top \Gamma_{X_2 X_1}^{(m)} \Gamma_{X_1}^{(m)-1} K(\mathbf{Z}_1) \right\|_{\mathbb{K}} \geq \frac{\lambda \tilde{w}_i}{4} \right\}.$$

We show that the probability of these events tends to zero when $N \rightarrow +\infty$. We start with $A_{i,1}$. We know that $\|K(Z_i)\|_{\mathbb{K}} \leq \theta_1 \|Z_i\|_{\mathbb{H}}$. In addition, from Theorem 1, for $i \in \mathcal{S}^{(m)c}$ there exists $C > 0$ such that

$$\sup_{i \notin \mathcal{S}^{(m)}} \left\| \tilde{\beta}_i^{(m)} \right\|_{\mathbb{K}} \leq Cr_N^{1/2}.$$

Using the definition of $\tilde{w}_i = \|\tilde{\beta}_i^{(m)}\|_{\mathbb{K}}^{-1}$, we find $\tilde{w}_i \geq 1/Cr_N^{1/2}$. This bound and Lemma 1 give:

$$\begin{aligned} P(A_{i,1}) &= P\left(N^{-1} \|Z_i\|_{\mathbb{H}} \geq \frac{\lambda \tilde{w}_i}{4\theta_1}\right) = P\left(N^{-1} \left\| \sum_{n=1}^N \epsilon_n X_{ni}^{(m)} \right\|_{\mathbb{H}} \geq \frac{\lambda \tilde{w}_i}{4\theta_1}\right) \\ &\leq \exp\left(-\frac{\lambda^2 \tilde{w}_i^2 N}{16\theta_1^2 M}\right) \leq \exp\left(-\frac{N\lambda^2}{16\theta_1^2 M C^2 r_N}\right). \end{aligned}$$

Now, let us move to $A_{i,2}$. Since

$$\left\| e_i^\top \Gamma_{X_2 X_1}^{(m)} \Gamma_{X_1}^{(m)-1} K(\mathbf{Z}_1) \right\|_{\mathbb{K}} \leq \theta_1 \varphi_m \|\mathbf{Z}_1\|_{\mathbb{H}} \leq \theta_1 \sum_{j \in \mathcal{S}^{(m)}} \|Z_j\|_{\mathbb{H}},$$

we can write

$$A_{i,2} \subseteq \bigcup_{j \in \mathcal{S}^{(m)}} \left\{ N^{-1} \|Z_j\|_{\mathbb{H}} \geq \frac{\lambda \tilde{w}_i}{4I_0\theta_1} \right\}.$$

With a similar argument as before,

$$P(A_{i,2}) \leq \sum_{j \in \mathcal{S}^{(m)}} \exp\left(-\frac{N\lambda^2 \tilde{w}_i^2}{16\theta_1^2 M I_0^2}\right) \leq I_0 \exp\left(-\frac{N\lambda^2}{16\theta_1^2 M I_0^2 C^2 r_N}\right).$$

Putting all things together, we have

$$P(A_i) \leq \exp\left(-\frac{N\lambda^2}{16\theta_1^2 M C^2 r_N}\right) + I_0 \exp\left(-\frac{N\lambda^2}{16\theta_1^2 M I_0^2 C^2 r_N}\right).$$

Therefore,

$$P(A_i) \leq (1 + I_0) \exp\left(-\frac{N\lambda^2}{16\theta_1^2 M \varphi_m^2 I_0^2 C^2 r_N}\right) \leq 2I_0 \exp\left(-\frac{N\lambda^2}{16\theta_1^2 M \varphi_m^2 I_0^2 C^2 r_N}\right).$$

From point 4 of Assumption 4, we know that $I_0^4 \log(I)^2/N^2 \ll \lambda^2$. Hence,

$$P(A_i) \leq 2I_0 \exp\left(-\frac{I_0^2 \log(I)^2}{16\theta_1^2 N M C^2 r_N}\right).$$

As to B_3 , we have

$$P(B_3) \leq \sum_{i \notin \mathcal{S}^{(m)}} p(A_i) \leq 2II_0 \exp\left(-\frac{I_0^2 \log(I)^2}{16\theta_1^2 NMC^2 r_N}\right) \leq \exp\left(-\frac{I_0^2 \log(I)^2}{16\theta_1^2 NMC^2 r_N} + \log(2II_0)\right).$$

Finally, from the definition of r_N in Corollary 1, we know that $r_N \ll I_0 \log(I)/N$. As a consequence,

$$\log(2II_0) \ll I_0 \log(I) \ll \frac{I_0^2 \log(I)^2}{Nr_N},$$

and this ensures that $P(B_3) \rightarrow 0$, $N \rightarrow +\infty$.

Step 4: $P(B_4) \rightarrow 0$, when $N \rightarrow +\infty$.

From eq. (19), and point 4 of Assumption 4, we can write:

$$\begin{aligned} P(B_4) &\leq \sum_{i \in \mathcal{S}^{(m)c}} P\left(N^{-1} \left\| e_i^\top \Gamma_{X_2 X_1}^{(m)} \Gamma_{X_1}^{(m)-1} \tilde{s}_1 \right\|_{\mathbb{K}} \geq \frac{\tilde{w}_i}{2}\right) \\ &\leq \sum_{i \in \mathcal{S}^{(m)c}} P\left(N^{-1} \|\tilde{s}_1\|_{\mathbb{K}} \geq \frac{\tilde{w}_i}{2\varphi_m}\right) \leq \sum_{i \in \mathcal{S}^{(m)c}} P\left(\frac{\|\tilde{s}_1\|_{\mathbb{K}}}{N\tilde{w}_i} \geq \frac{1}{2}\right). \end{aligned}$$

Another use of the expression (19) gives $\tilde{w}_i^{-1} = O_P(r_N^{1/2})$ for any $i \in \mathcal{S}^{(m)c}$. Thus, with probability tending to 1,

$$\frac{\|\tilde{s}_1\|_{\mathbb{K}}}{N\tilde{w}_i} \ll \frac{I_0 \sqrt{\log(I)}}{b_m \sqrt{N}}.$$

At this point, point 2 of Assumption 4 proves that $P(B_4) \rightarrow 0$, when $N \rightarrow +\infty$.

(ii). So far, we have shown that, with probability tending to 1, $\hat{\mathcal{S}}^{(m)} = \mathcal{S}^{(m)}$ and in this case, the estimation takes the form $\hat{\beta}^{(m)} = (\hat{\beta}_1^{(m)}, 0)$. From eq. (15) we know that

$$\hat{\beta}_1^{(m)} = \beta_1^{*(m)} + N^{-1} \Gamma_{X_1}^{(m)-1} (K(\mathbf{Z}_1) - \lambda \tilde{s}_1). \quad (20)$$

The oracle estimator is given by $\hat{\beta}^{O(m)} = (\hat{\beta}_1^{O(m)}, 0)$, where $\hat{\beta}_1^{O(m)} = \Gamma_{X_1}^{(m)-1} \Gamma_{Y X_1}^{(m)}$. A simple calculation shows that

$$\hat{\Gamma}_{Y X_1}^{(m)} = \frac{1}{N} \sum_{n=1}^N Y_n K(X_{ni}^{(m)}) = \Gamma_{X_1}^{(m)} (\beta_i^*) + N^{-1} \Gamma_{X_1}^{(m)-1} K(\mathbf{Z}_1).$$

As a result,

$$\hat{\beta}_1^{O(m)} = \beta_1^{*(m)} + N^{-1} \Gamma_{X_1}^{(m)-1} K(\mathbf{Z}_1).$$

Combining eq. (20) and the latter, we obtain

$$\hat{\beta}_1^{O(m)} - \hat{\beta}_1^{(m)} = \lambda N^{-1} \Gamma_{X_1}^{(m)-1} \tilde{s}_1.$$

We now analyze $\|\hat{\beta}_1^{O(m)} - \hat{\beta}_1^{(m)}\|_{\mathbb{K}}$:

$$\begin{aligned} \sqrt{N} \left\| \hat{\beta}_1^{O(m)} - \hat{\beta}_1^{(m)} \right\|_{\mathbb{K}} &= \sqrt{N} \left\| N^{-1} \lambda \Gamma_{X_1}^{(m)-1} \tilde{s}_1 \right\|_{\mathbb{K}} \leq \frac{\lambda}{\tau_m \sqrt{N}} \|\tilde{s}_1\|_{\mathbb{K}} \\ &\leq \frac{\lambda}{\tau_m \sqrt{N}} \cdot \frac{N \sqrt{I_0} \theta_1}{b_m} (1 + o_p(1)) \\ &= \frac{\theta_1}{\tau_m} \lambda \frac{\sqrt{N} \sqrt{I_0}}{b_m} (1 + o_p(1)) = o_p(1), \end{aligned}$$

where the last equality is true by point 4 of Assumption 4.

(iii) First observe that

$$\sqrt{N} \left\| \hat{\beta}_1^{(m)} - \hat{\beta}_1^* \right\|_{\mathbb{K}} \leq \sqrt{N} \left\| \hat{\beta}_1^{(m)} - \hat{\beta}_1^{O(m)} \right\|_{\mathbb{K}} + \sqrt{N} \left\| \hat{\beta}_1^{O(m)} - \beta_1^* \right\|_{\mathbb{K}}.$$

In this equation, we already proved that the first term on the right-hand side converges to zero in probability, as $N \rightarrow +\infty$. Regarding the second term, we compute the expected value and use Markov's inequality. For all $i \in \mathcal{S}^{(m)}$ and $j \in \mathbb{N}$,

$$\begin{aligned} \mathbb{E} \left(\left\langle \hat{\beta}_i^{O(m)}, v_j \right\rangle_{\mathbb{K}} \right) &= \mathbb{E} \left(\left\langle \beta_i^{*(m)} + e_i \Gamma_{X_1}^{(m)-1} (Z_1), v_j \right\rangle_{\mathbb{K}} \right) \\ &= \mathbb{E} \left(\left\langle \beta_i^{*(m)}, v_j \right\rangle_{\mathbb{K}} \right) + \mathbb{E} \left(\left\langle e_i \Gamma_{X_1}^{(m)-1} \left(X_1^{(m)\top} \epsilon \right), v_j \right\rangle_{\mathbb{K}} \right) \\ &= \left\langle \beta_i^{*(m)}, v_j \right\rangle_{\mathbb{K}}, \end{aligned}$$

where the last equality holds because the design matrix is deterministic and ϵ is sub-Gaussian with mean zero. So,

$$\mathbb{E} \left(\left\langle \hat{\beta}_i^* - \hat{\beta}_i^{O(m)}, v_j \right\rangle_{\mathbb{K}} \right) = \left\langle \beta_i^{*(m)\perp}, v_j \right\rangle_{\mathbb{K}}.$$

Now we apply Markov's inequality. For any $\delta > 0$,

$$\begin{aligned} P \left(N \left\| \hat{\beta}_i^* - \hat{\beta}_i^{O(m)} \right\|_{\mathbb{K}}^2 > \delta \right) &= P \left(\left\| \hat{\beta}_i^* - \hat{\beta}_i^{O(m)} \right\|_{\mathbb{K}} > \frac{\delta}{N} \right) = P \left(\sum_{j=1}^{+\infty} \left\langle \hat{\beta}_i^* - \hat{\beta}_i^{O(m)}, v_j \right\rangle_{\mathbb{K}}^2 > \frac{\delta}{N} \right) \\ &\leq \frac{N^2}{\delta^2} \mathbb{E} \left(\sum_{j=1}^{+\infty} \left\langle \hat{\beta}_i^* - \hat{\beta}_i^{O(m)}, v_j \right\rangle_{\mathbb{K}}^2 \right) \leq \frac{N^2}{\delta^2} \left(\sum_{j=1}^{+\infty} \left\langle \hat{\beta}_i^{*(m)\perp}, v_j \right\rangle_{\mathbb{K}}^2 \right) \\ &\leq \frac{N^2}{\delta^2} \left\| \hat{\beta}_i^{*(m)\perp} \right\|_{\mathbb{K}}^2. \end{aligned}$$

This means that $N \left\| \hat{\beta}_i^* - \hat{\beta}_i^{O(m)} \right\|_{\mathbb{K}}^2 = o_p(I_0^{-1})$ for all $i \in \mathcal{S}^{(m)}$. Finally,

$$\sqrt{N} \left\| \hat{\beta}_1^* - \hat{\beta}_1^{O(m)} \right\|_{\mathbb{K}} = \sum_{i \in \mathcal{S}^{(m)}} \left(N \left\| \hat{\beta}_i^* - \hat{\beta}_i^{O(m)} \right\|_{\mathbb{K}}^2 \right)^{\frac{1}{2}} \leq I_0 I_0^{-1} o_p(1) = o_P(1).$$

Thus, the second term in eq. (A.6) tends to zero when $N \rightarrow +\infty$. This completes the proof.

B RE condition

In the following proposition, we show that, if we assume that the correlation between null predictors tends to zero with a fast rate, then the RE condition is satisfied under Assumption 4.

Proposition 3. *Let points 1 and 3 of Assumptions 4 hold. Assume that*

$$\tau_m^{-1} > 9I_0 \sigma_{\max} \left(\Gamma_{X_2}^{(m)} \right) + 6\sqrt{I_0} \sigma_{\max} \left(\Gamma_{X_2}^{(m)} \right) \varphi_m.$$

Then, there exists $k_m > 0$ such that, for any $\delta \in \mathbb{K}^{(m)I}$ with $\|\delta_{\mathcal{S}^{(m)C}}\|_{\ell_1/\mathbb{K}} \leq 3\|\delta_{\mathcal{S}^{(m)}}\|_{\ell_1/\mathbb{K}}$, we have $\|\Gamma_{XX}^{(m)1/2} \delta\| \geq k_m \|\delta\|$.

Proof. Let $\boldsymbol{\delta} \in \mathbb{K}^{(m)}$ such that $\|\boldsymbol{\delta}_{\mathcal{S}^{(m)C}}\|_{\ell_1/\mathbb{K}} \leq 3\|\boldsymbol{\delta}_{\mathcal{S}^{(m)}}\|_{\ell_1/\mathbb{K}}$. First, observe that

$$\begin{aligned} \left\| \Gamma_{XX}^{(m)1/2}(\boldsymbol{\delta}) \right\|_{\mathbb{K}} &= \left\langle \Gamma_{XX}^{(m)}(\boldsymbol{\delta}), \boldsymbol{\delta} \right\rangle_{\mathbb{K}} = \left\langle \Gamma_{X_1}^{(m)}(\boldsymbol{\delta}_{\mathcal{S}^{(m)}}), \boldsymbol{\delta}_{\mathcal{S}^{(m)}} \right\rangle_{\mathbb{K}} \\ &\quad + \left\langle \Gamma_{X_2}^{(m)}(\boldsymbol{\delta}_{\mathcal{S}^{(m)C}}), \boldsymbol{\delta}_{\mathcal{S}^{(m)C}} \right\rangle_{\mathbb{K}} + 2 \left\langle \Gamma_{X_2X_1}^{(m)}(\boldsymbol{\delta}_{\mathcal{S}^{(m)C}}), \boldsymbol{\delta}_{\mathcal{S}^{(m)C}} \right\rangle_{\mathbb{K}}. \end{aligned}$$

We bound all the terms on the left-hand side. For the first one, we use point 1 of Assumption 4:

$$\left\langle \Gamma_{X_1}^{(m)}(\boldsymbol{\delta}_{\mathcal{S}^{(m)}}), \boldsymbol{\delta}_{\mathcal{S}^{(m)}} \right\rangle_{\mathbb{K}} \geq \tau_m^{-1} \|\boldsymbol{\delta}_{\mathcal{S}^{(m)}}\|^2.$$

For the second one, we can write

$$\begin{aligned} \left\langle \Gamma_{X_2}^{(m)}(\boldsymbol{\delta}_{\mathcal{S}^{(m)C}}), \boldsymbol{\delta}_{\mathcal{S}^{(m)C}} \right\rangle_{\mathbb{K}} &\leq \sigma_{max}(\Gamma_{X_2}^{(m)}) \|\boldsymbol{\delta}_{\mathcal{S}^{(m)C}}\|^2 \leq \sigma_{max}(\Gamma_{X_2}^{(m)}) \|\boldsymbol{\delta}_{\mathcal{S}^{(m)C}}\|_{\ell_1/\mathbb{K}}^2 \\ &\leq 9 \sigma_{max}(\Gamma_{X_2}^{(m)}) \|\boldsymbol{\delta}_{\mathcal{S}^{(m)}}\|_{\ell_1/\mathbb{K}}^2 \leq 9 I_0 \sigma_{max}(\Gamma_{X_2}^{(m)}) \|\boldsymbol{\delta}_{\mathcal{S}^{(m)}}\|^2. \end{aligned}$$

Finally, for the third one, we have

$$\begin{aligned} 2 \left\langle \Gamma_{X_1X_2}^{(m)}(\boldsymbol{\delta}_{\mathcal{S}^{(m)C}}), \boldsymbol{\delta}_{\mathcal{S}^{(m)}} \right\rangle_{\mathbb{K}} &= 2 \left\langle \Gamma_{X_1}^{(m)} \Gamma_{X_1}^{(m)-1} \Gamma_{X_1X_2}^{(m)}(\boldsymbol{\delta}_{\mathcal{S}^{(m)C}}), \boldsymbol{\delta}_{\mathcal{S}^{(m)}} \right\rangle_{\mathbb{K}} \\ &\leq 2 \sigma_{max}(\Gamma_{X_1}^{(m)}) \left\| \Gamma_{X_1}^{(m)-1} \Gamma_{X_1X_2}^{(m)} \right\|_{op} \|\boldsymbol{\delta}_{\mathcal{S}^{(m)}}\| \|\boldsymbol{\delta}_{\mathcal{S}^{(m)C}}\|_{\ell_1/\mathbb{K}} \\ &\leq 6 \sigma_{max}(\Gamma_{X_1}^{(m)}) \varphi_m \|\boldsymbol{\delta}_{\mathcal{S}^{(m)}}\|_{\ell_1/\mathbb{K}}^2 \leq 6 \sqrt{I_0} \sigma_{max}(\Gamma_{X_1}^{(m)}) \varphi_m \|\boldsymbol{\delta}_{\mathcal{S}^{(m)}}\|^2. \end{aligned}$$

Now, by summing all the bounds and using the triangle inequality,

$$\begin{aligned} \left\| \Gamma_{XX}^{(m)1/2}(\boldsymbol{\delta}) \right\| &\geq \left\langle \Gamma_{X_1}^{(m)}(\boldsymbol{\delta}_{\mathcal{S}^{(m)}}), \boldsymbol{\delta}_{\mathcal{S}^{(m)}} \right\rangle_{\mathbb{K}} - \left\langle \Gamma_{X_2}^{(m)}(\boldsymbol{\delta}_{\mathcal{S}^{(m)C}}), \boldsymbol{\delta}_{\mathcal{S}^{(m)C}} \right\rangle_{\mathbb{K}} - 2 \left\langle \Gamma_{X_2X_1}^{(m)}(\boldsymbol{\delta}_{\mathcal{S}^{(m)C}}), \boldsymbol{\delta}_{\mathcal{S}^{(m)C}} \right\rangle_{\mathbb{K}} \\ &\geq \left(\tau_m^{-1} - 9 I_0 \sigma_{max}(\Gamma_{X_2}^{(m)}) - 6 \sqrt{I_0} \sigma_{max}(\Gamma_{X_1}^{(m)}) \varphi_m \right) \|\boldsymbol{\delta}_{\mathcal{S}^{(m)}}\|^2. \end{aligned}$$

Therefore, we obtain the desired result by defining

$$k_m = \tau_m^{-1} - 9 I_0 \sigma_{max}(\Gamma_{X_2}^{(m)}) - 6 \sqrt{I_0} \sigma_{max}(\Gamma_{X_1}^{(m)}) \varphi_m.$$

□

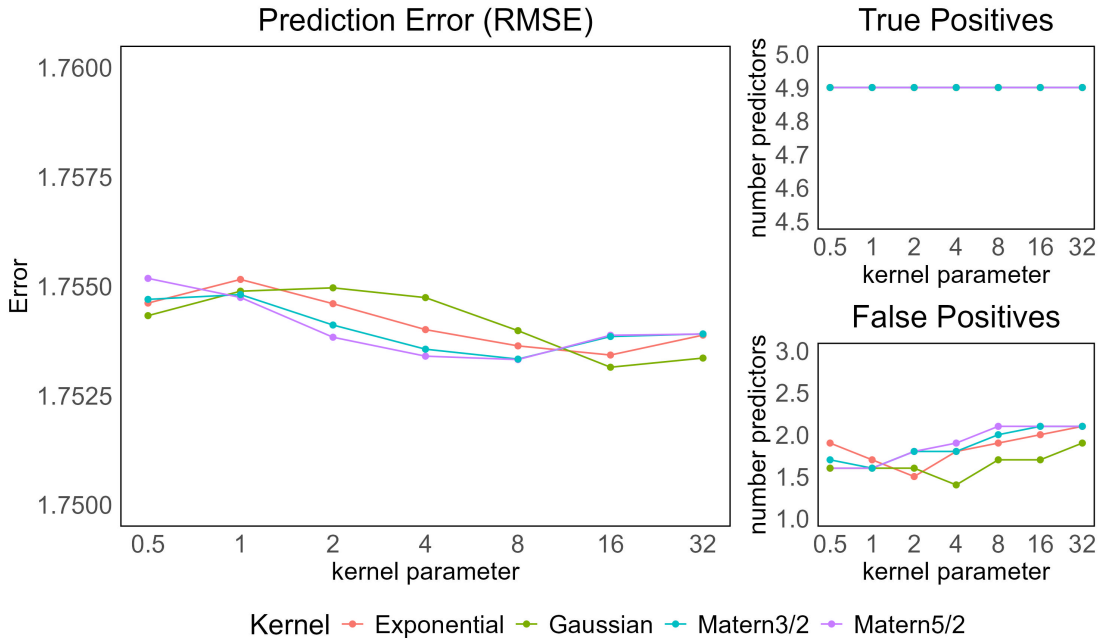
C Appendix C. Additional figures

To provide a comprehensive perspective, we include the boundary noise scenarios of the simulation study in this appendix.

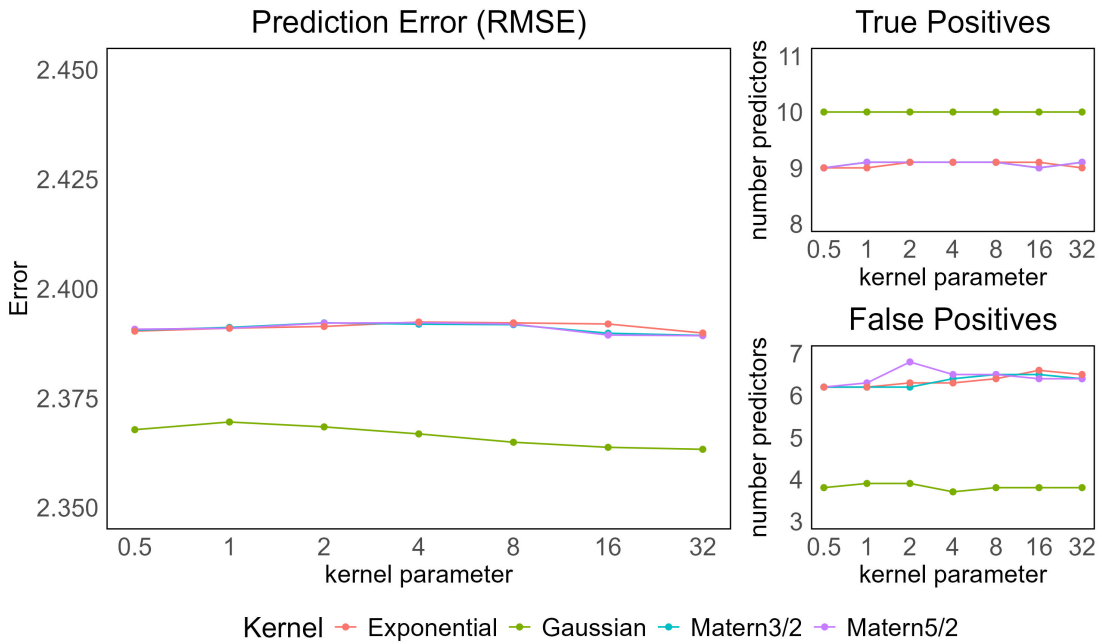
Figure 5 illustrates the impact of high noise. False positive rates increase, and RMSE values rise, particularly under the difficult regime. While all kernel functions exhibit comparable performance in this challenging setting, the Gaussian kernel tends to achieve slightly lower false positive rates, suggesting better robustness to noise. Figure 6 highlights the near noise-free setting, where SOFIA achieves optimal performance with exact support recovery and minimal prediction error across all kernels and both regimes.

These figures demonstrate that SOFIA adapts well to a wide range of noise conditions, maintaining accurate prediction and stable variable selection even under high-dimensional, high-noise functional regression scenarios.

SNR = 0.5



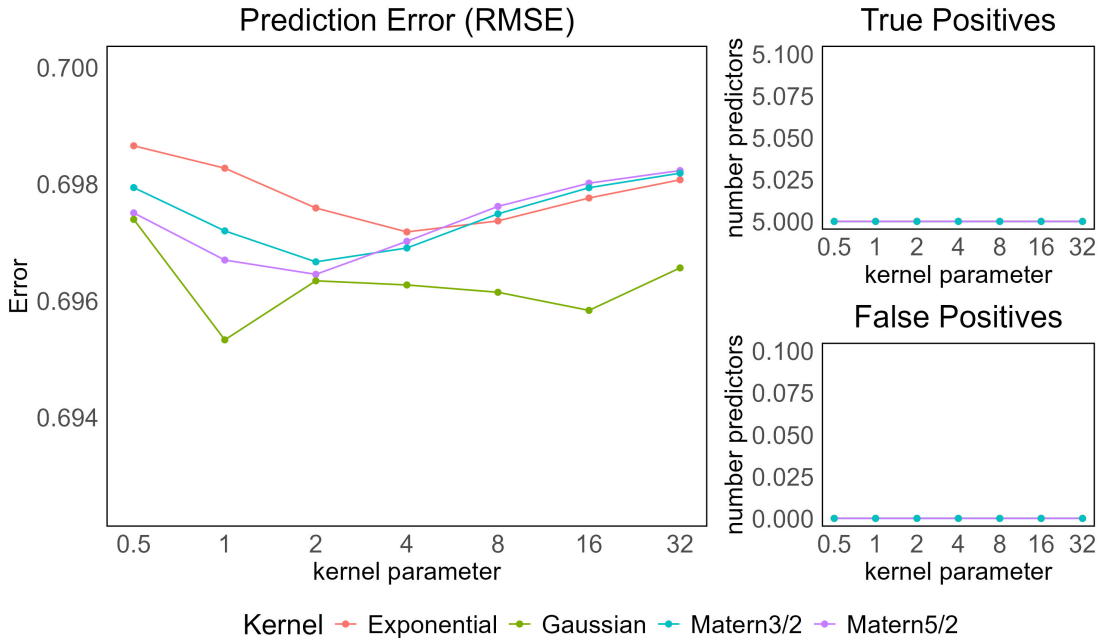
(a) Easy regime



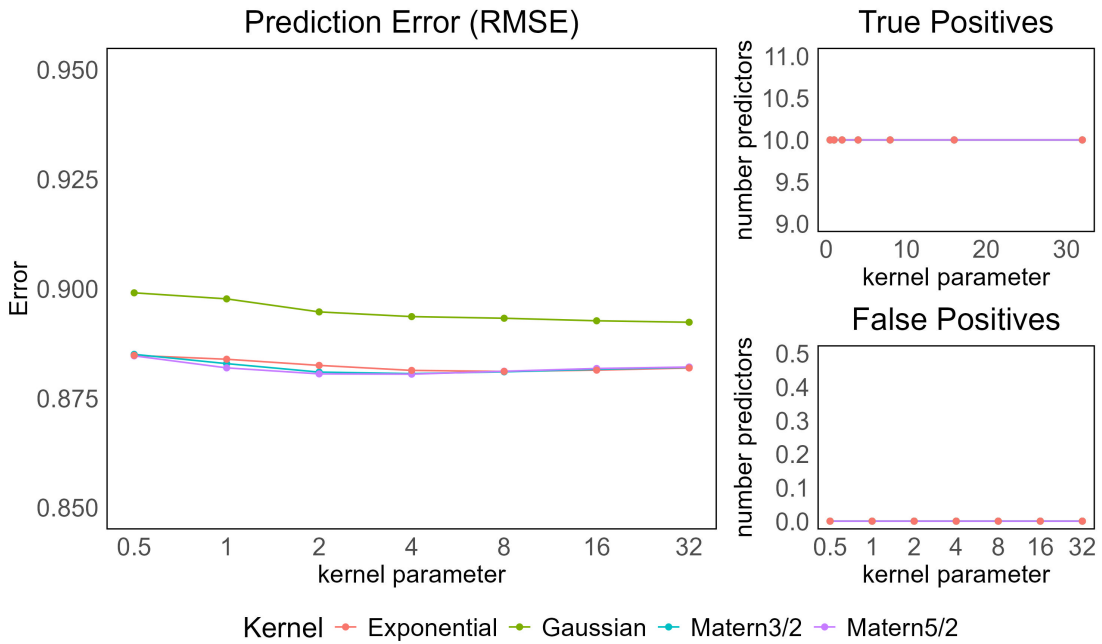
(b) Difficult regime

Figure 5: Comparison of the performance of different kernels under varying parameter values for SNR = 0.5. Each subfigure shows the true positive rate, false positive rate, and root mean squared error (RMSE) in one regime.

SNR = 100



(a) Easy regime



(b) Difficult regime

Figure 6: Comparison of the performance of different kernels under varying parameter values for SNR = 100. Each subfigure shows the true positive rate, false positive rate, and root mean squared error (RMSE) in one regime.

References

- Aneiros, G., S. Novo, and P. Vieu (2022). Variable selection in functional regression models: A review. *Journal of Multivariate Analysis* 188, 104871.
- Barber, R. F., M. Reimherr, and T. Schill (2017). The function-on-scalar LASSO with applications to longitudinal GWAS. *Electronic Journal of Statistics* 11, 1351–1389.
- Bauschke, H. H., P. L. Combettes, et al. (2011). *Convex Analysis and Monotone Operator Theory in Hilbert Spaces*, Volume 408. Springer.
- Bellec, P. and A. Tsybakov (2017). Bounds on the prediction error of penalized least squares estimators with convex penalty. In *Modern Problems of Stochastic Analysis and Statistics: Selected Contributions In Honor of Valentin Konakov*, pp. 315–333. Springer.
- Berlinet, A. and C. Thomas-Agnan (2011). *Reproducing Kernel Hilbert Spaces in Probability and Statistics*. Springer Science & Business Media.
- Berrendero, J. R., B. Bueno-Larraz, and A. Cuevas (2019). An RKHS model for variable selection in functional linear regression. *Journal of Multivariate Analysis* 170, 25–45.
- Bickel, P. J., Y. Ritov, and A. B. Tsybakov (2009). Simultaneous analysis of Lasso and Dantzig selector. *The Annals of Statistics* 38(4), 1705—1732.
- Boschi, T., L. Testa, F. Chiaromonte, and M. Reimherr (2024). FASTen: an efficient adaptive method for feature selection and estimation in high-dimensional functional regressions. *Journal of Computational and Graphical Statistics*, 1–24.
- Boucheron, S., G. Lugosi, and O. Bousquet (2013). Concentration inequalities. In *Summer School on Machine Learning*, pp. 208–240. Springer.
- Bühlmann, P. and S. Van De Geer (2011). *Statistics for High-dimensional Data: Methods, Theory, and Applications*. Springer Science & Business Media.
- Cardot, H., C. Crambes, and P. Sarda (2007). Ozone pollution forecasting using conditional mean and conditional quantiles with functional covariates. *Statistical methods for biostatistics and related fields*, 221–243.
- Fan, J. and R. Li (2001). Variable selection via nonconcave penalized likelihood and its oracle properties. *Journal of the American Statistical Association* 96(456), 1348–1360.
- Fan, Y., G. M. James, and P. Radchenko (2015). Functional additive regression. *The Annals of Statistics* 43(5), 2296–2325.
- Fan, Z. and M. Reimherr (2017). High-dimensional adaptive function-on-scalar regression. *Econometrics and Statistics* 1, 167–183.
- Fortin-Gagnon, O., M. Leroux, D. Stevanovic, and S. Surprenant (2022). A large Canadian database for macroeconomic analysis. *Canadian Journal of Economics* 55(4), 1799–1833.
- Genton, M. G. (2001). Classes of kernels for machine learning: a statistics perspective. *Journal of Machine Learning Research* 2(Dec), 299–312.
- Gertheiss, J., A. Maity, and A.-M. Staicu (2013). Variable selection in generalized functional linear models. *Stat* 2(1), 86–101.
- Hanke, M., L. Dijkstra, R. Foraita, and V. Didelez (2024). Variable selection in linear regression models: Choosing the best subset is not always the best choice. *Biometrical Journal* 66(1), 2200209.

- Hsing, T. and R. Eubank (2015). *Theoretical Foundations of Functional Data Analysis, with an Introduction to Linear Operators*, Volume 997. John Wiley & Sons.
- Huang, J., S. Ma, and C.-H. Zhang (2008). Adaptive lasso for sparse high-dimensional regression models. *Statistica Sinica* 18, 1603–1618.
- Huang, L., J. Zhao, H. Wang, and S. Wang (2016). Robust shrinkage estimation and selection for functional multiple linear model through LAD loss. *Computational Statistics & Data Analysis* 103, 384–400.
- Insolia, L., A. Kenney, F. Chiaromonte, and G. Felici (2022). Simultaneous feature selection and outlier detection with optimality guarantees. *Biometrics* 78(4), 1592–1603.
- Kadri, H., E. Duflos, P. Preux, S. Canu, and M. Davy (2010). Nonlinear functional regression: a functional RKHS approach. In *Proceedings of the Thirteenth International Conference on Artificial Intelligence and Statistics*, pp. 374–380. JMLR Workshop and Conference Proceedings.
- Kapetanios, G., M. Marcellino, and F. Papailias (2016). Forecasting inflation and GDP growth using heuristic optimisation of information criteria and variable reduction methods. *Computational Statistics & Data Analysis* 100, 369–382.
- Kokoszka, P. and M. Reimherr (2017). *Introduction to Functional Data Analysis*. Chapman and Hall/CRC.
- Lian, H. (2013). Shrinkage estimation and selection for multiple functional regression. *Statistica Sinica* 23, 51–74.
- Lounici, K., M. Pontil, S. Van De Geer, and A. B. Tsybakov (2011). Oracle inequalities and optimal inference under group sparsity. *The Annals of Statistics* 39(4), 2164–2204.
- Matsui, H. and S. Konishi (2011). Variable selection for functional regression models via the L_1 regularization. *Computational Statistics & Data Analysis* 55(12), 3304–3310.
- Mirshani, A. and M. Reimherr (2021). Adaptive function-on-scalar regression with a smoothing elastic net. *Journal of Multivariate Analysis* 185, 104765.
- Murphy, G. J. (1990). *C*-Algebras and Operator Theory*. San Diego: Academic Press.
- Parodi, A. and M. Reimherr (2018). Simultaneous variable selection and smoothing for high-dimensional function-on-scalar regression. *Electronic Journal of Statistics* 12(2), 4602–4639.
- Paulsen, V. I. and M. Raghupathi (2016). *An Introduction to the Theory of Reproducing Kernel Hilbert Spaces*, Volume 152. Cambridge University Press.
- Ramsay, J. O. and B. W. Silverman (2005). *Functional Data Analysis* (2 ed.). Springer.
- Roche, A. (2023). Lasso in infinite dimension: application to variable selection in functional multivariate linear regression. *Electronic Journal of Statistics* 17(2), 3357–3405.
- Sarason, D. (2007). *Complex Function Theory* (2 ed.). American Mathematical Society.
- Shin, H. and S. Lee (2016). An RKHS approach to robust functional linear regression. *Statistica Sinica* 26(1), 255–272.
- Ullah, S. and C. F. Finch (2013). Applications of functional data analysis: A systematic review. *BMC medical research methodology* 13, 1–12.
- Wang, D., Z. Zhao, Y. Yu, and R. Willett (2022). Functional linear regression with mixed predictors. *Journal of Machine Learning Research* 23(266), 1–94.

- Widom, H. (1964). Asymptotic behavior of the eigenvalues of certain integral equations. II. *Archive for Rational Mechanics and Analysis* 17(3), 215–229.
- Yuan, M. and T. T. Cai (2010). A reproducing kernel Hilbert space approach to functional linear regression. *The Annals of Statistics* 38(6), 3412–3444.
- Zhang, X., Y. Huang, K. Xu, and L. Xing (2023). Novel modeling strategies for high-frequency stock trading data. *Financial Innovation* 9(1), 39.
- Zhao, P. and B. Yu (2006). On model selection consistency of lasso. *The Journal of Machine Learning Research* 7, 2541–2563.
- Zou, H. (2006). The adaptive lasso and its oracle properties. *Journal of the American Statistical Association* 101(476), 1418–1429.